Cadmium Telluride Solar Cell: From Device Modeling to Battery Charging Application

through Maximum Power Point Tracking and Charging Circuitry

Khalid Nazmus Sakib

A Thesis

In the Department

Of

Electrical and Computer Engineering

Presented in Partial Fulfillment of the Requirements

For the Degree of Master of Applied Science at

Concordia University

Montréal Québec Canada

July 2013

CONCORDIA UNIVERSITY SCHOOL OF GRADUATE STUDIES

This is to certify that the thesis prepared

By: Khalid Nazmus Sakib

Entitled: "Cadmium Telluride Solar Cell: From device modeling to battery charging application through maximum power point tracking and battery charging circuitry" and submitted in partial fulfillment of the requirements for the degree of

Master of Applied Science

Complies with the regulations of this University and meets the accepted standards with respect to originality and quality.

Signed by the final Examining Committee:

_____ Chair
  Dr. Abdelwahab Hamou-Lhadj

_____ Supervisors
 Dr. Sheldon Williamson and Dr. M. Z. Kabir

_____ Examiner
  Dr. Ashutosh Bagchi

_____ Examiner
  Dr. Mojtaba Kahrizi

Approved by ———————————————————
  Dr. W. E. Lynch.
  Chair, Department of Electrical and Computer Engineering

July 2013
       _____
        Dr. Christopher Trueman
        Dean, Faculty of Engineering and
        Computer Science

ABSTRACT

Cadmium Telluride Solar Cell: From Device Modeling to Battery Charging Application through Maximum Power Point Tracking and Charging Circuitry

Khalid Nazmus Sakib

Battery charging for industrial and vehicular application by second generation thin film solar cells like CdTe can have a promising future for their cheaper production and better efficiency. Though the production of solar cells is still based mainly on silicon (Si), the market share of thin film solar has been increasing over the last few years. The mathematical modeling of the voltage dependent current-voltage (I-V) characteristics of Cadmium Telluride (CdS/CdTe) Solar cell and utilizing the model as an electrical source to charge a Li-ion battery and to charge it a battery charging algorithm in a concept level has been analyzed in this thesis. A single cell is developed based on the mathematical model and a solar module/network is constructed considering a series and parallel combinations of the single cell. The module performance is analyzed from efficient circuit operating viewpoint under various operating conditions. To extract the power from the solar cell, Perturb and Observe (P&O) Maximum power point technique has been used. Battery charging with its charging algorithm is also discussed in this paper. To apply the power as charging source after P&O converter a second dc-dc converter driven with a battery charging algorithm is applied to charge a Li-ion battery. A simple charging algorithm considering both constant current and constant voltage mode charging system has been developed. Both CC and CV mode and algorithm switching between these two modes developed here has shown a consistent result in battery charging simulation.

ACKNOWLEDGMENTS

Contents

List of Figures

List of Tables

List of Abbreviations

PV - Photo Voltaic

Cd - Cadmium

a-Si - amorphous silicon

CdTe - Cadmium Telluride

CdS - Cadmium Sulfide

CIS - Copper Indium Selenide

SnO_2 – Tin Oxide

ITO / In_2O_3:Sn - Indium Tin Oxide

TCO – Transparent Conducting Oxide

NERL - National Renewable Energy Laboratory

AM - Air Mass

MPP – Maximum Power Point Tracking

P&O – Perturb and Observed

Ni-Cd – Nickel Cadmium

Ni-MH - Nickel Metal Hydride

Li-Ion - Lithium Ion

SOC – State of Charge

CCM - continuous conduction mode

CC - Constant Current

CV- Constant Voltage

IGBT - Insulated Gate Bipolar Transistor

MOSFET - Metal Oxide Semiconductor Field Effect Transistor

List of Principal Symbols

p - Hole concentration

$\alpha(\lambda)$ - The absorption coefficient of CdTe

λ - The photon wavelength

x - The depth in the CdTe layer

$G(\lambda)$ - Electron-hole pair or carrier generation rate

$j_e(\lambda,V)$, $j_h(\lambda,V)$ - Photo current density for electrons and hole drifting

t_h, t_e - The normalized carrier lifetime of hole and electron

τ_h', τ_e' - Carrier lifetime of hole and electron

μ_h, μ_e - Hole and electron mobility

Δ - The normalized absorption depth

$\alpha_1(\lambda)$ - The absorption coefficient of CdS layer

d - The CdS layer thickness

c – The speed of light

h - The Planck constant

I_0 - The intensity of the solar spectra (W/cm^2/nm)

R - The total reflection and other loss factor

$J_L(V)$ - Total photo generated

$F(V)$ - The external voltage dependent electric field

$J_d(V)$ - The forward diode current

n_i - The intrinsic carrier concentration of CdTe

J_0 - The reverse saturation current density of the p–n junction

A - The diode ideality factor

k - The Boltzman constant

T - The absolute temperature

V_0 - The flat-band voltage

R_s - Series Resistance

V_T - Thermal Voltage

N_s - Number of series cells

N_p - Number of parallel cells

D – Duty Cycle

V_{in} - Input voltage to the dc-dc converter

V_o - Output voltage of the dc-dc converter

L_{min} - Minimum inductance for the converter

C_{min} - Minimum inductance for the converter

N_C, N_V - effective density state function in the conduction band and valence band

E_g - Direct band gap energy

Chapter 1: Introduction

1.1 Thin Film solar cell and prospect of CdTe among them

The second-generation thin film solar cells are increasingly promising for their cheaper production and better efficiency. Though the production of solar cells is still based mainly on silicon (Si), the market share of thin film solar has been increasing over the last few years in 2010 [1]. Among various thin film solar cells cadmium telluride (CdTe) thin-film solar cell is the fastest growing commercial photovoltaic, which captured 13% of global market [1]. The CdTe solar cell has a superstrate structure of glass-substrate/ITO/SnO$_2$/CdS/CdTe/metal [2][3] as shown in Figure 1.1.

Light

Glass Substrate	
ITO (In$_2$O$_3$:Sn)	Transparent
SnO$_2$(Tin dioxide)	conducting oxide (TCO)
n-Cds	Window layer
p-CdTe	Absorber
Ni-Al Metal Contact	
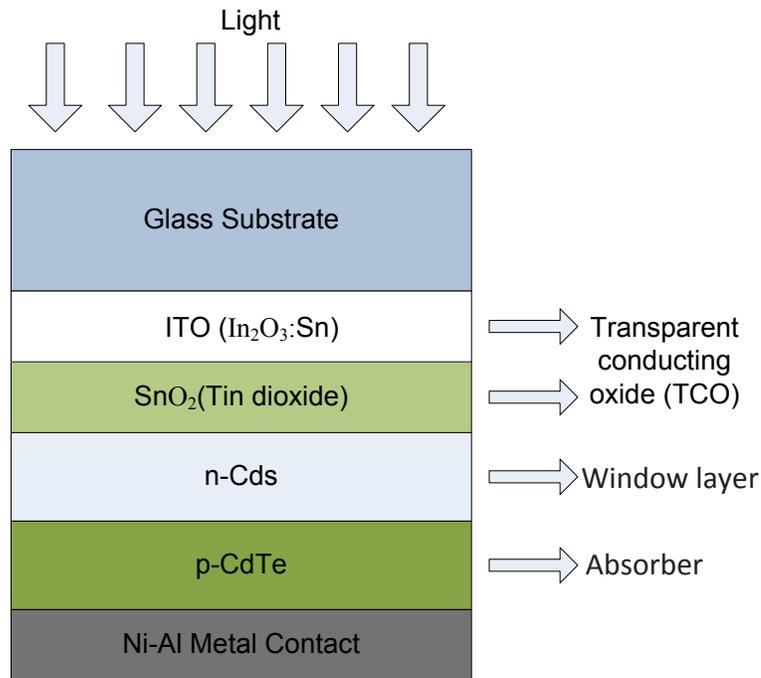
Figure 1.1: Device structure of Thin Film Cds/CdTe solar cell

The cell has a p-n heterojunction structure where a very thin layer (~0.1 μm) of CdS acts as a very highly doped n-layer and CdTe acts as a very lightly doped p-layer that also act as a light absorbing layer. The photons are mainly absorbed in the CdTe layer. As this layer is fully deplated the photocarriers are collected by the built-in electric field in this layer. The voltage dependent charge collection in CdTe layer is the dominant charge collection mechanisms in this thin film solar cells [3][4].
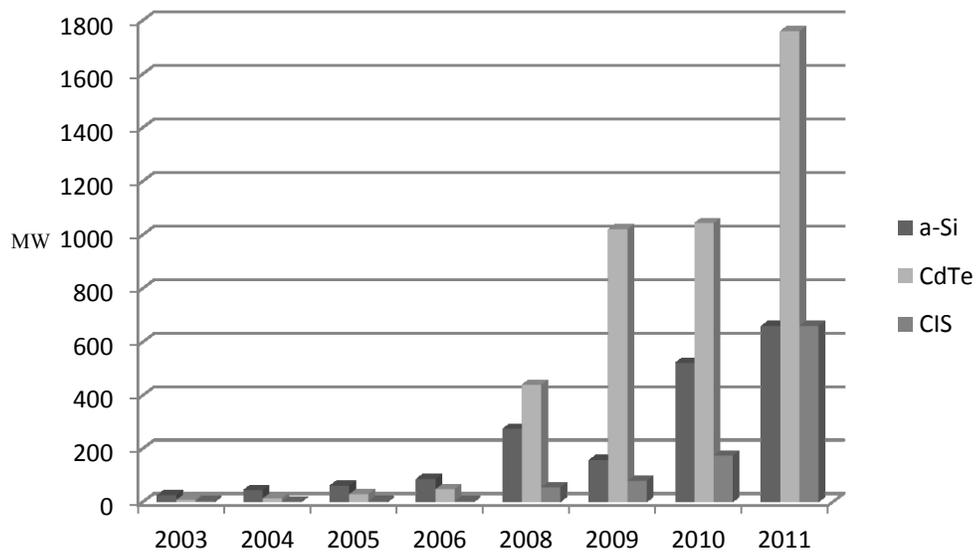
Figure 1.2: Production rate (MW) of different types of thin film solar cells

As shown in Figure 1.2, the rapidly growing production rates for popular manufacturers of these thin-film technologies over the past 3 years are dominated by the cadmium telluride solar cells [5][6][7]. There are several number of PV technologies. Some of them are commercially available and others are under development. They can be classified into three groups also referred to as 1st, 2nd and 3rd generation: 1st generation -

wafer-based crystalline silicon(c-Si); 2nd generation - Thin-films (TF); and 3rd generation emerging and novel PV technologies, including concentrating PV, organic PV, advanced thin films and other novel concepts. Since the production associated with the wafer-based techniques are increasing very fast, the market associated with thin-film technology based solar cells have to grow in quick pace to maintain their present market share. The main barrier to penetrate market for thin-film technologies is higher capital costs per unit output for thin-film manufacturing facilities.

On the other hand the manufacturing drawback of the conventional wafer-based crystalline solar cell modules is that it generally consists of four separately-financed operations: 1. silicon purification, 2. crystal growth and wafering 3. Cell processing and 4. Cell encapsulation. But in a thin-film operation, all these operations effectively are compact into the one facility. So, even though the thin film based production does not have those problems if they do meet up with present demand of solar cell market, there could be chance to capture those markets by wafer based crystalline Si technology.

1.2 Cadmium Telluride (CdS/CdTe) Solar cell

Various types of thin film solar cells are described in [8]. Cadmium telluride devices are fabricated preferably in the superstrate configuration because the CdTe surface is exposed for contacting. Cadmium telluride solar cells use borosilicate glass for high temperature deposition (600 ∘C) and soda lime glass for low temperature deposition (60–500 ∘C). Cadmium telluride has also been deposited on thin metallic foils such as stainless steel, Mo, Ni and Cu. One simple structure that a CdTe solar cell can have is a structure of

glass/ SnO₂/CdS/CdTe/metal. Cds acts as n type substrate and CdTe acts as a p type substrate.

CdTe is a polycrystalline material. Polycrystalline CdTe is very well suited for using as active material in thin-film solar cells. It has an energy gap of 1.45eV, and therefore is well adapted to the spectrum of solar radiation. The CdS layer is much thinner and knows as buffer layer.
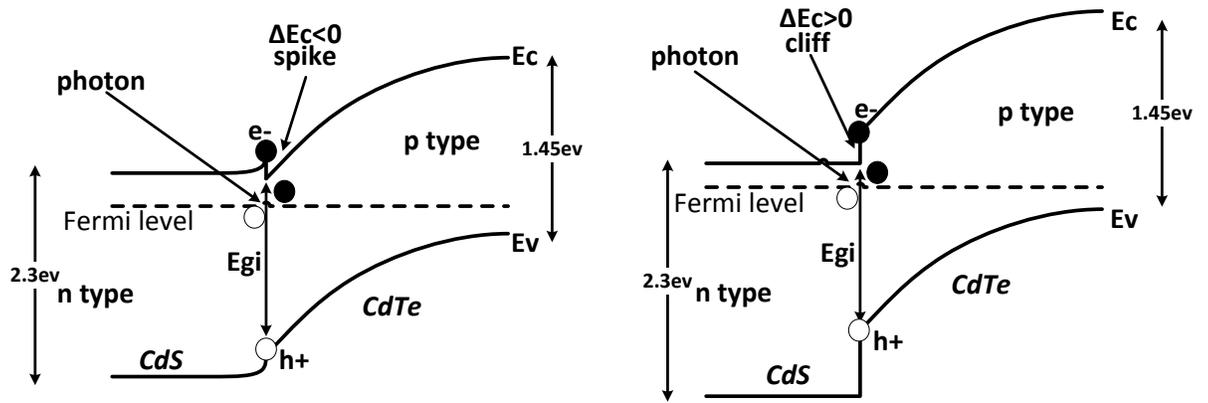
Figure 1.3: Energy band diagrams of CdS/CdTe solar cell structure.

The energy band diagram of CdS/CdTe solar cell is shown in Figure 1.3. The junction is formed by contacting two different semiconductors - CdS and CdTe. From the figure we can see when a photon is absorbed an electron/hole pair is generated. The CdTe layer is almost depleted and the generated electron hole pairs are separated by the built-in electric field causing quanta of charge to flow through an external load. The misalignment in the conduction bands can be calculated by electron affinity of both materials which is $\Delta E_c = E_C^{CdTe} - E_C^{CdS} = \chi^{CdS} - \chi^{CdTe}$[8]. If ΔE_c is too negative, there is a 'cliff' means the CB of CdTe is above the CB of CdS at the junction. This decreases the open circuit

Voltage. If ΔE_c is too positive, there is a 'spike' means the CB of CdTe is below the CB of CdS at the junction. This decreases the short circuit current. A cliff of less than 0.2 eV is observed in this structure.

1.3 Cell efficiency

Before R&D research started at First Solar, the best cell efficiency has recorded was 16.5% by US Department of Energy's National Renewable Energy Laboratory (NERL) [9].
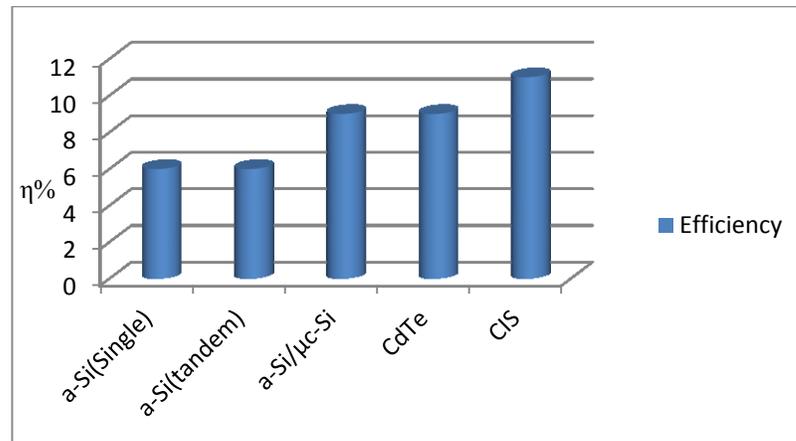
Figure 1.4: Efficiency of different type of thin film solar cells (2006)

Figure 1.4 is showing the cell level efficiency of different thin film solar cells. New R&D test cells produced at First Solar's Perrysburg, Ohio factory and R&D center have reached a new record cell conversion efficiency of 18.7% [10]. The record was also verified by the NREL and announced by First Solar very recently.

It has been over a year since First Solar announced in July 2011 that it had achieved a record cell efficiency of 17.3%, which was then surpassed by rival GE with a reported cell efficiency of 18.3% [10].

Quality doping of CdTe and better understanding of carrier transport and parameter realization are key to improving cell efficiency. As CdTe has the optimal band gap for single-junction devices, it should be expected that efficiencies close to exceeding 20% and can be achievable.

1.4 Low Cost Manufacturing

The most attractive advantage of CdTe solar cell is that the panels can be manufactured at lower costs than silicon based solar cells. As showed the record, "First Solar" was the first manufacturing company of CdTe solar panels to produce solar cells for less than a dollar per watt [11].

Some expect that it would be possible to get the solar cell costs down to around $0.5 per watt in near future. When there is sufficient sunlight CdTe panels and networks would allow producing electricity in the $0.06 to $0.08 / kWh range that is less than a fuel based electricity cost [11].

1.5 Advantages of Cadmium Telluride Solar Panels

Advantages of CdTe solar cells over traditional silicon technology include:

1. Simpler manufacturing process: In CdTe solar cell the necessary electric field that turns solar energy into electricity, generated from properties of two types of cadmium compound molecules which are Cadmium Sulfide (CdS) and Cadmium Telluride (CdTe). A simple mixture of these two types of molecules achieves the required properties, which is much simpler than the manufacturing compared to the multistep process to join two different types of doped silicon in a silicon solar cell.

2. Matching with sunlight energy: CdTe solar cell absorbs sun at close to the ideal wavelength and capture energy at shorter wavelengths than that with the silicon panels.

3. Abundance of CdTe: Cadmium is abundant, produced as a byproduct of important industrial metals such as zinc. Also it never showed the wider price swings that happen sometimes in case of Silicon which would greatly affect the market and production estimation.

1.6 Disadvantages

While price is a major advantage, there are some disadvantages to this type of solar panels. [11]

1. Tellurium supply: Tellurium is not that much abundant like Cadmium. Tellurium (Te) is a rare element. It is available as a by-product of copper, lead and gold. 1 GW of CdTe PV modules would require about 93 metric tons at current efficiencies and thicknesses. So the availability of tellurium may limit the number of panels that can be produced with this material.

As tellurium availability is significant in PV's future impact on global energy research is going on to counter this impact. Recently, researchers mostly astrophysicists identify tellurium abundantly available with the element with an atomic number over 40 like tin, bismuth, and lead. Researchers have also shown that well known undersea ridges are rich in tellurium and it could supply more tellurium than we could ever use for our global energy.

2. Toxicity of Cadmium: Cadmium is one of the toxic materials known. However, the compound CdTe is less toxic than the Cadmium itself.

CdTe is toxic if its dust is inhaled or ingested or if it is handled improperly without appropriate gloves and other safety measurement. The toxicity is not solely due to the cadmium content. Other than the toxicity of CdTe, in the time of recrystallization of telluride films, cadmium chloride is used which is also toxic.

But in the large scale commercialization of cadmium telluride solar panels the disposal and long term safety precaution of cadmium telluride is ensured. In fact recycling the modules at the end of their useful life which is generally 25 to 30 years resolves any environmental concerns. Also it is important to note that during their operation, these solar cells do not cause any pollution. Furthermore, as they can be used as an alternative to the fossil fuels, they can offer a great environmental benefit. Also it is worth mentioning that the use of Cd in PV is more environmentally friendly than other uses currently associated with Cd.

1.7 Motivation

The batteries related to electric vehicle or hybrid electric vehicles can be charged overnight from renewable sources such as wind and solar energy but these charging systems include power electronic, converters, batteries, ultra-capacitors, sensors, and micro-controllers [12]. Also the energy storage units must be sized so that they store sufficient kWh and provide adequate peak power (kW) to have a specified acceleration and the capability to meet the driving cycles to satisfy the requirement in real world driving [13]. Almost all the hybrid topologies [14] the quality of the charging system plays a key role in life and reliability of the battery. All the energy in a battery electric vehicle (BEV) that drives the vehicle is stored and carried in batteries [15]. Therefore, Battery management system has major consequences for the vehicle design and performance.
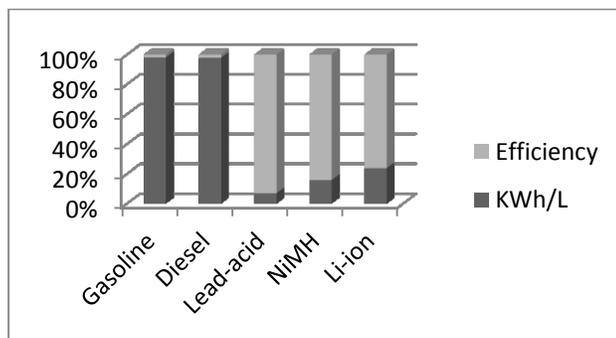
Figure 1.5:Vehicle mass and efficiency as two compromising factor when choosing energy storage in EVs [15]
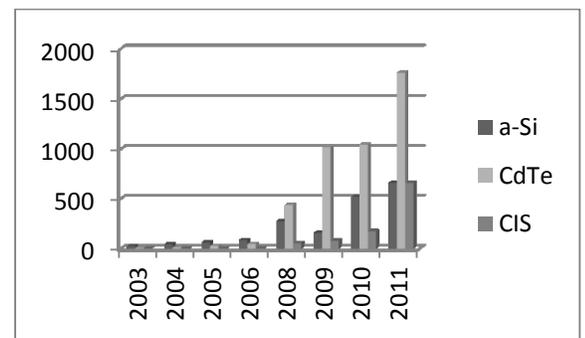
Figure 1.6: Production rate (MW) of different types of thin film solar cells

We can see from Figure 1.4 that petrol and diesel give much more kWh/L while their efficiency is much lower comparing that to the batteries. For a conventional car the energy transfer by gasoline and diesel is thousand times faster comparing to charge a Battery EV even when considering level 3 DC fast charging (50 kW). Therefore, hybrid

plugin vehicle comes in to play which can use both electric and gasoline/diesel energy when needed. Typical HEV contains the internal combustion engine with a secondary energy storage device such as a battery, fuel cell or ultra-capacitor. This hybrid arrangement is more fuel-efficient than conventional one and, at the same time, is more environment-friendly [14]. As evident from Figure 1.6, CdTe could be a favorable position to choose when charging the battery with solar energy. Therefore, we developed the concept of battery charging with CdTe Solar cell and simulated the charging system to back up the whole concept.

The mathematical modeling we used would also be capable of taking account the effect of shading and temperature changing. This is also one of the reasons to simulate the system with this kind of easy to manipulate modeling. Also when charging algorithm works with the maximum power point tracking algorithm driving two different dc-dc converters with two different topologies mismatch between these two algorithms might have happened [16]. Therefore the possibility of this mismatch is included in the simulation and possible solutions are proposed.

1.8 Research Objectives

- Establishing the way and technique to implement the modeling mathematics into circuit action and developing the array from single cell with the data and the parameters published in several articles and papers.

- Implementing Maximum power point algorithm and integrate it with solar cell taking account of both intensity and temperature change and the effect on the current voltage curve hence on the Maximum Power point

- Developing and implementing the charging algorithm in a simple dc-dc converter circuit for a Li-ion Battery which is capable of describing and depicting the constant charging and constant voltage charging and their switching transition and condition with simulation and algorithm

- Finding the optimum preset value by targeting the end of charge or by state of charge detection

1.9 Organization of the thesis

There are 7 chapters in the thesis. They are described below.

- Chapter 1 consists of the motivation behind the thesis and also contains the description of the CdTe solar cell. It describes the different aspects of CdTe solar cell and cell efficiency, advantages and disadvantages. The chapter also contains the present market share of CdTe cell comparing with the share of other technologies. It explains the possibilities and advantages of using CdTe solar cells in vehicle standard battery charging where in general at present Si based solar cell is being used in the case.

- Chapter 2 has contained the theory and modeling of the CdTe single solar cell. It also described the technique and requirements to develop an instantaneous electric source.

- Chapter 3 has described the detailed development of the PV array from the single source. It also characterized the parameters collected from different literatures. It also

described the Maximum Power point tracking system and complete implementation of the circuit from the mathematics and the derived current voltage characteristics.

- Chapter 4 has contained all the battery basics and charging parameter definitions which are characterized in the consecutive chapters. It described some end of charge detection method which would be a very important parameter when implementing the algorithm in a practical way.

- Chapter 5 has described the charging algorithm and the description of the dc-dc converters driven by that algorithm. Based on the charging scheme (constant voltage and constant current) and charging rate (slow, quick and fast) described in chapter 4 algorithm is designed to charge the Li-ion battery with a quick charging rate of C/2.

- Chapter 6 contains the simulation result discussions. Array response to temperature and intensity change is flowed by maximum power point tracking algorithm developed. Single cell characteristics are verified with the experimental data. Solar cell characteristics change as a function of CdTe width and temperature change are described. Charging characteristics as charging voltage, charging current and charging voltage vs state of charge are illustrated and explained and matched with the typical charging characteristics.

- Chapter 7 contains the conclusion, publications, and future works and about the improvements and complexity of the improvements of the algorithm and circuit.

Chapter 2:   Theory and cell modeling

An analytical expression for voltage dependent photocurrent has been developed by solving continuity equation for electrons and holes. Electron-hole pair generation is considered exponential as photons are absorbed exponentially. Load current is consists of forward bias diode current and the light illuminated photocurrent. Electron hole pairs are created in CdTe absorber layer by Sunlight, and these photo-generated electrons and holes are drifted towards top and bottom contacts respectively. Some assumptions are made in the modeling. Thermal equilibrium carriers are considered negligibly small, CdTe is fully depleted, built-in Electric field F is uniform or constant, carrier diffusion is negligible comparing to carrier drift as CdTe fully depleted, holes and electrons have same life time τ', constant drift mobility μ.

From this model a single cell is developed based on the mathematical model and a solar module/network is constructed considering a series and parallel combinations of the single cell. The module performance is analyzed under various operating conditions. To operate the circuit in Maximum power point Perturb and Observe (P&O) Maximum power point technique has been used [17][18]. Instead of using a simple resistive load a battery with charge controller with dc-dc boost converter would be used in battery charging.

2.1 Modeling Current Voltage Characteristics

In the proposed model [19] as in the real scenario the Cds layer has a very short diffusion length and very thin width. So, the photon absorption in the highly doped CdS layer will contribute a negligible current. That is why the photo generated electrons and holes are drifted in opposite directions mainly by the built-in electric field in the CdTe layer. Electrons drift towards the radiation-receiving contact (top contact) and holes drift towards the bottom contact. An analytical expression for the external voltage dependent photocurrent is derived in [20] by solving the continuity equation for both electrons and holes [19]. There are few theoretical models [21]. The solution process used here starts with the Steady State continuity equation. If we write the continuity equation for holes, it suggests as,

$$\frac{\partial p}{\partial t} = -\mu_h F \frac{\partial p}{\partial x} - \frac{p}{\tau'_h} + G e^{-\alpha x}$$

$$= 0 \qquad\qquad\qquad (2.1)$$

Where $\alpha(\lambda)$ is the absorption coefficient of CdTe, λ is the photon wavelength, x is the depth in the CdTe layer from the n–p interface, G is the carrier generation rate at x=0, p is the hole concentration. The subscript h refers to holes. Taking initial condition p(x=0) =0 the solution of the equation (2.1) is,

$$p(x, \lambda) = \frac{G\tau'_h}{1 - \alpha\mu_h F\tau'_h}\left(e^{-\alpha x} - e^{\frac{-x}{\mu_h F\tau'_h}}\right) \qquad\qquad (2.2)$$

Now the photo current density for holes drifting towards bottom contact,

$$j_h(\lambda, V) = \frac{e\mu_h F}{W}\int_0^W p(x, \lambda)\, dx \qquad\qquad (2.3)$$

$$j_h(\lambda, V) = eGW\left\{(\tau_h^{-1} - \Delta^{-1})^{-1}\left[\Delta\left(1 - e^{-\frac{1}{\Delta}}\right) - \tau_h\left(1 - e^{-\frac{1}{\tau_h}}\right)\right]\right\} \tag{2.4}$$

Similarly we can find the photo current density $j_e(\lambda, V)$ for electrons drifting towards the top contact and the total current thus we can find is

$$j_e(\lambda, V) = \frac{-e\mu_e F}{W}\int_0^w n(x, \lambda)\,dx \tag{2.5}$$

$$j_e(\lambda, V) = eGW\left\{(\tau_e^{-1} - \Delta^{-1})^{-1}\left[\Delta\left(1 - e^{-\frac{1}{\Delta}}\right) - \tau_e\left(e^{-\frac{1}{\Delta}} - e^{-\frac{1}{\Delta} - \frac{1}{\tau_e}}\right)\right]\right\} \tag{2.6}$$

So the total light current,

$$j_L(\lambda, V) = eGW\left\{(\tau_h^{-1} - \Delta^{-1})^{-1}\left[\Delta\left(1 - e^{-\frac{1}{\Delta}}\right) - \tau_h\left(1 - e^{-\frac{1}{\tau_h}}\right)\right]\right.$$
$$\left. + (\tau_e^{-1} - \Delta^{-1})^{-1}\left[\Delta\left(1 - e^{-\frac{1}{\Delta}}\right) - \tau_e\left(e^{-\frac{1}{\Delta}} - e^{-\frac{1}{\Delta} - \frac{1}{\tau_h}}\right)\right]\right\} \tag{2.7}$$

Where $\tau_e = \mu_e \tau_e' F/W$ and $\tau_h = \mu_h \tau_h' F/W$, e is the elementary charge, W is the depth of the CdTe layer, Δ is the normalized absorption depth where $\Delta = 1/(\alpha W)$, t_h is the normalized carrier lifetime (carrier lifetime per unit transit time) for holes. Since F is voltage dependent, t_h is voltage dependent and so does j_h.

The electron-hole pair generation rate,

$$G(\lambda) = \frac{\alpha(\lambda)e^{-\alpha_1(\lambda)d}(1 - R(\lambda))\lambda I_0(\lambda)}{hc} \tag{2.8}$$

Where $\alpha_1(\lambda)$ is the absorption coefficient of CdS layer, d is the CdS layer thickness, c is the speed of light, h is the Planck constant, I_0 is the intensity of the solar spectra

15

(W/cm^2/nm), and R is the total reflection and other loss factor. The other losses include shading, absorption in the top SnO$_2$ layer, and incomplete EHP generation in the CdTe layer.

The total photo generated current density is obtained by integrating over all incident photon wavelengths of the solar spectra,

$$J_L(V) = \int_0^{\infty} j_L(\lambda, V) d\lambda \qquad (2.9)$$

The net current density from a single cell is

$$J(V) = J_L(V) - J_d(V) \qquad (2.10)$$

Where $J_d(V)$ is the forward diode current.

The external voltage dependent electric field is given by [3],

$$F(V) = \frac{V_0 - V_j}{W} = \frac{V_0 - (V - JR_s)}{W} \qquad (2.11)$$

Where R_s is the effective series resistance including all contact resistances, V_j (=V − JR$_s$) is the junction voltage, and V_0 is the flat-band voltage so that $J_L(V) = 0$ at $(V - JR_s) = V_0$ [20].

The forward diode current density,

$$J_d(V) = J_0 exp\left[\frac{e(V - JR_s)}{AkT}\right] \qquad (2.12)$$

Where J_0 is the reverse saturation current density of the p–n junction, A is the diode ideality factor, k is the Boltzman constant, and T is the absolute temperature. For the thick depletion region and $V >> V_t$ the reverse saturation current density can be written as [19]

$$J_0 \approx \frac{\pi e n_i W V_t}{2\sqrt{\tau_e' \tau_h'}(V_{bi} - V)} \qquad (2.13)$$

Here n_i is intrinsic carrier concentration of CdTe.

2.2 Implementing Modeling Mathematics in Circuit

To implement the mathematics in circuit level we first calculated,

$$J_L(V) = \int_0^\infty j_L(\lambda, V)d\lambda$$

$$= \int_0^\infty eGW \left\{ (\tau_h^{-1} - \Delta^{-1})^{-1} \left[\Delta\left(1 - e^{-\frac{1}{\Delta}}\right) - \tau_h\left(1 - e^{-\frac{1}{\tau_h}}\right) \right] \right.$$

$$\left. + (\tau_e^{-1} - \Delta^{-1})^{-1} \left[\Delta\left(1 - e^{-\frac{1}{\Delta}}\right) - \tau_e\left(e^{-\frac{1}{\Delta}} - e^{-\frac{1}{\Delta} - \frac{1}{\tau_e}}\right) \right] \right\} d\lambda \qquad (2.14)$$

To derive this we need the relations between $\alpha(\lambda)$, the absorption coefficient of CdTe and $\alpha_l(\lambda)$, the absorption coefficient of CdS layer with λ that has been shown in Figure 2.1 [8].
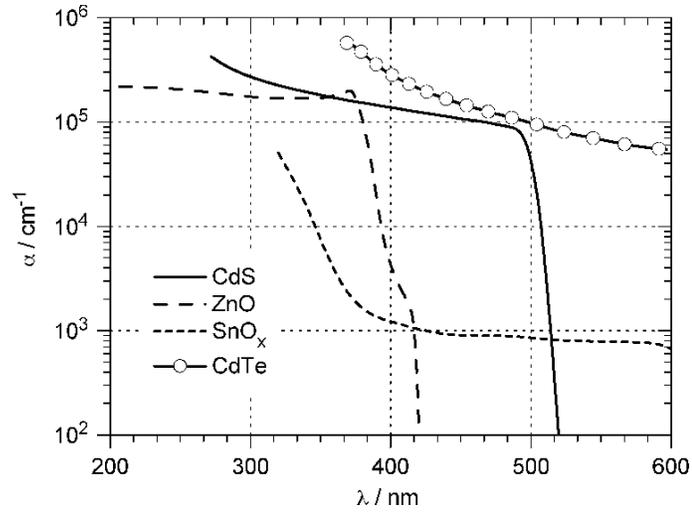
Figure 2.1: Optical absorption coefficient of the absorber, buffer and window layer for CdTe solar cell [8]

The analytical expression for the absorption coefficients are also given in Ref. [22]. The absorption coefficients using the expression of Ref. [22] are plotted in Figure 2.2.
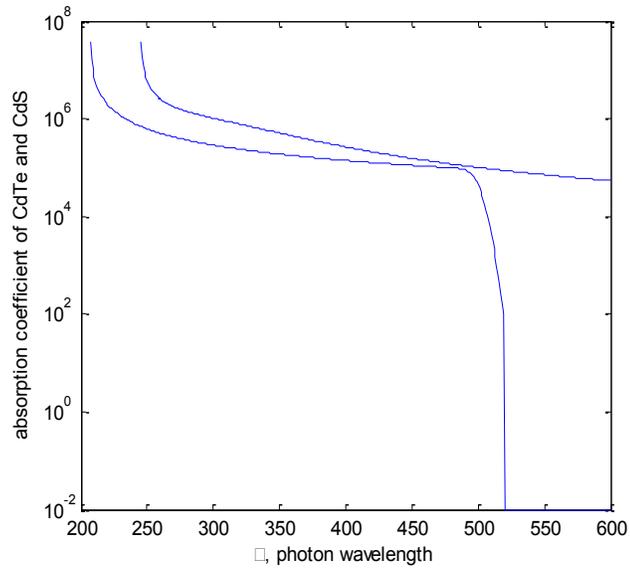
Figure 2.2: Optical absorption coefficient of the CdTe and CdS

The incident photon flux intensity is taken for (AM) 1.5 Global spectrums [23], which are shown in Figure 2.3.

18

ASTM G173-03 Reference Spectra
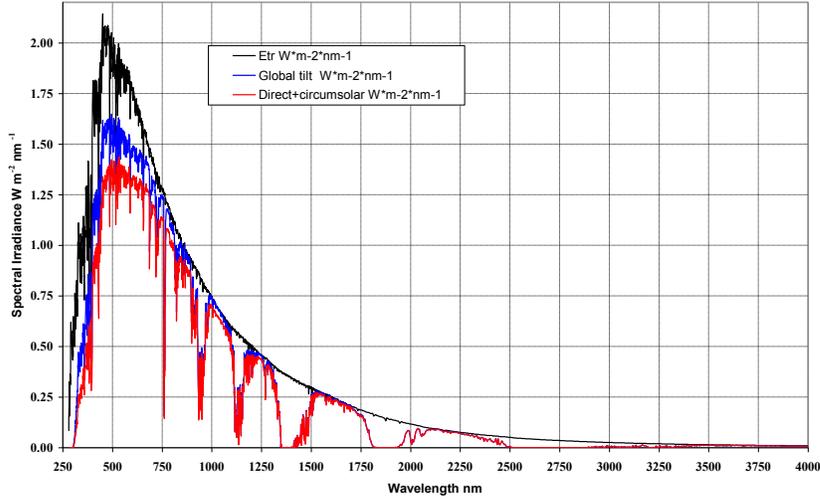
Figure 2.3: Spectral Irradiance Vs wavelengths

To get $J_L(V)$, from a non-linear equation, $J(V) = J_L(V) - J_d(V)$ that means

$$J_L(V) = \int_0^\infty e \times \frac{\alpha(\lambda)e^{-\alpha_1(\lambda)d}(1 - R(\lambda))\lambda I_0(\lambda)}{hc}$$

$$\times W \left\{ (\tau_h^{-1} - \Delta^{-1})^{-1} \left[\Delta \left(1 - e^{-\frac{1}{\Delta}} \right) - \tau_h \left(1 - e^{-\frac{1}{\tau_h}} \right) \right] \right.$$

$$+ (\tau_e^{-1} - \Delta^{-1})^{-1} \left. \left[\Delta \left(1 - e^{-\frac{1}{\Delta}} \right) - \tau_e \left(e^{-\frac{1}{\Delta}} - e^{-\frac{1}{\Delta} - \frac{1}{\tau_e}} \right) \right] \right\} d\lambda$$

$$- \frac{\pi e n_i W V_t}{2\sqrt{\tau_e' \tau_h'}(V_{bi} - V)} \times \frac{e(V - JR_s)}{AkT} \qquad (2.15)$$

Where, $\tau_e = \mu_e \tau_e' F/W$, $\tau_h = \mu_h \tau_h' F/W$ and

$$F(V) = \frac{V_0 - V_j}{W} = \frac{V_0 - (V - JR_s)}{W}$$

Where R_s is the effective series resistance including all contact resistances, V_j ($=V$ $- JR_s$) is the junction voltage, and V_0 is the flat-band voltage so that $J_L(V) = 0$ at ($V - JR_s$) $= V_0$

The forward diode current density,

$$J_d(V) = J_0 exp \left[\frac{e(V - JR_s)}{AkT} \right]$$

Where J_0 is the reverse saturation current density of the p–n junction, A is the diode ideality factor, k is the Boltzmann constant, and T is the absolute temperature. For the thick depletion region and $V \gg V_t$ the reverse saturation current density can be written as [19]

$$J_0 \approx \frac{\pi e n_i W V_t}{2\sqrt{\tau_e' \tau_h'}(V_{bi}-V)}$$

Where ni is the intrinsic carrier concentration of CdTe.

The circuit model of single cell is shown in Figure 2.4.
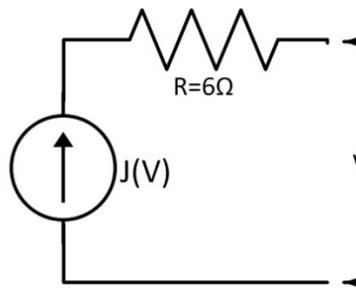
Figure 2.4: A single solar cell

To make circuit calculation faster, $\alpha_1(\lambda)$, $\alpha(\lambda)$, $G(\lambda)$, $\Delta(\lambda)$ are calculated outside the circuit and used as a matrix values when implemented the current source for the solar cell.

2.3 Current Voltage Characteristics

The J-V characteristics of the CdS/CdTe solar cells are calculated by iteratively solving equation 2.1 to 2.13. Incident photon flux $I_0(\lambda)$ is taken as the air mass (AM) 1.5 global spectrum from the ASTM G-173-03 standard [23]. The absorption coefficients for CdTe and CdS are obtained from the absorption curves in Ref. [8] as mentioned before. The J-V characteristics for different intensities are shown in Figure 2.5. The parameters for the J-V characteristics are given in Table 6.1. The maximum power points shift with the change of irradiances. Figure 2.6 shows the different power curve due to intensity change over time for shading and other reasons.
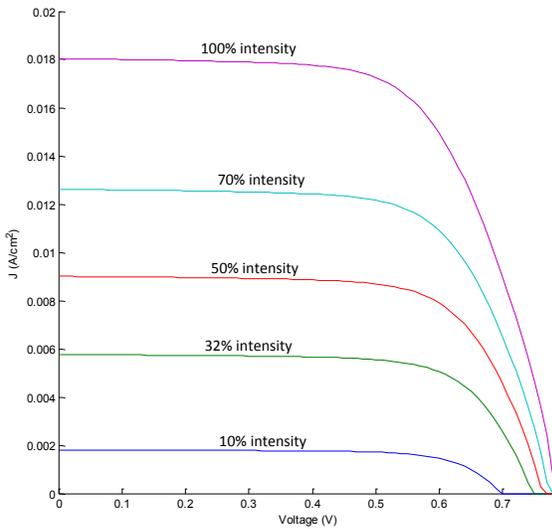
Figure 2.5: Current Voltage characteristics at different intensities
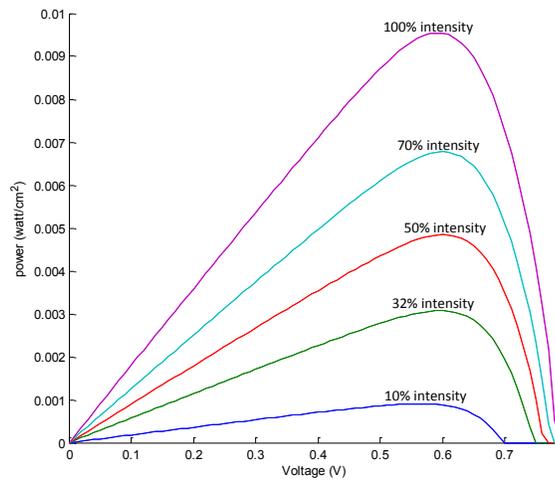
Figure 2.6: Power vs Voltage characteristics at different intensities

The electron-hole pairs are mainly generated at near the junction at CdTe layer near junction. Therefore, electron travels a shorter distance and move quickly towards top contact while holes move a longer distance and need more time to reach the bottom contact. Therefore, current density is mainly controlled by hole transport. This we can see by changing $\mu_h\tau_h'$ and $\mu_e\tau_e'$ Products as described in [19].

Chapter 3:   Modeling PV array and Circuit implementation

3.1 Modeling the PV Array

If we compare the ideal equation of the PV cell, $I = I_{pv,cell} - I_{0,cell} \left[e^{-\left(\frac{qV}{akT}\right)} - 1 \right]$ where $I_{pv,cell}$ is the current generated by the incident light $I_{0,cell}$ is the reverse saturation or leakage current of the diode, with Equation 12 we can say that $J_L(V) \approx I_{pv,cell}$ and $J_d(V) \approx I_{0,cell} \left[e^{-\left(\frac{qV}{akT}\right)} - 1 \right]$. Following the procedure mentioned in [24] to model the PV array for CdTe solar cell the thermal voltage of the array should be changed as $V_T = N_s \frac{kT}{e}$, where N_s is the number of cells connected in series. But we devided the array voltage by number of series cells and use the single cell model to get the characterestics of the array, do need not change V_T. Cells that are connected in parallel add the current and cells that are connected in series add output voltages from the solar cell. If the array is composed of Np number of parallel cells, the PV current or the light current and the saturation current or the dark current can be expressed as $I_{pv} = I_{pv,cell} N_p$ and $I_0 = I_{0,cell} N_p$.
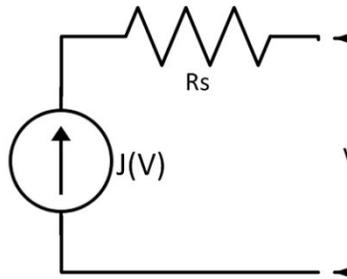
Figure 3.1: A single solar cell

The equivalent circuit models for series and parallel cells are shown in Figure 3.2 and Figure 3.3.
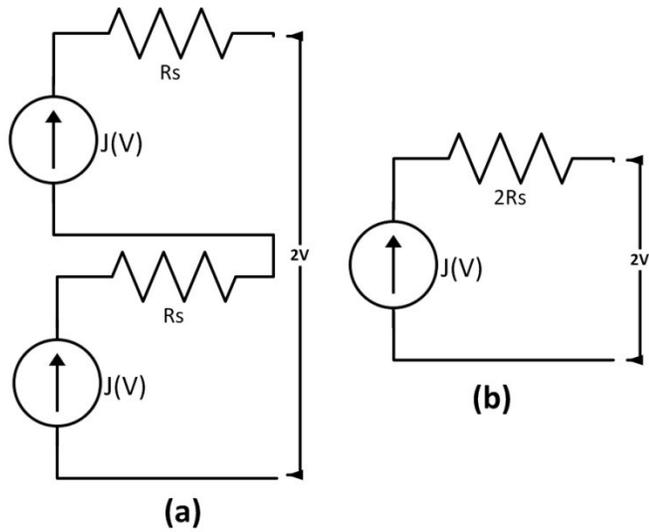
Figure 3.2: (a) 2 solar cells in series and (b) their equivalent circuit
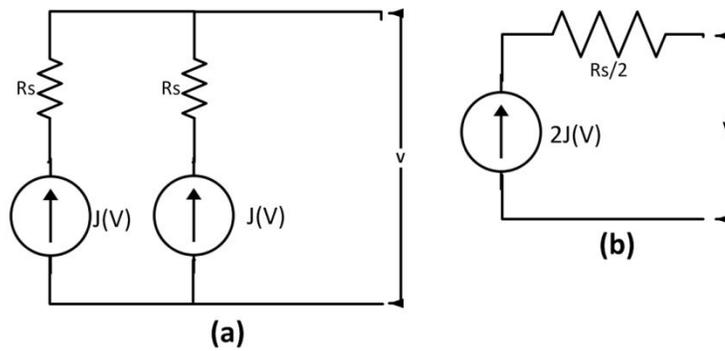
Figure 3.3: (a) 2 solar cells in parallel (b) their Equivalent circuit

Therefore, the external voltage is the sum of the cell voltages of all the series cells and the external current is the sum of the cell currents of all the parallel cells.

Commercially CdTe solar cell is available on $25cm^2$ glass substrate [25]. Present day CdTe modules as mentioned in [26] can have ~$1m^2$ in area. We have used $25cm^2$ for each of cell in our model according to [3] [25].

3.2 Maximum Power Point Tracking

There are several ways we can track the maximum power point from the power coming out from a PV cell. We can use various algorithms such as Perturb and Observe (P&O), Incremental Conductance, Open Circuit Voltage and Short Circuit Current. P&O is simpler method and Incremental Conductance is the extension of P&O. In our case, we used Perturb and Observe (P&O) to extract the power form the Solar cell.

3.3 Perturb and Observe (P&O)

The "perturb and observe (P&O)" algorithm, is based on the observation of the array output power and on the perturbation i.e. increment or decrement of the power based on increments of the array voltage or current. The P&O technique continuously changes the reference current or voltage based on the value of sample power measured at the previous step. The P&O is the simplest method which senses the PV array voltage and power and act upon the system to reach the maximum point. The cost of the implementation of this technique is less and hence easy to implement. Though the time complexity of this algorithm is very less, it doesn't step at the MPP on reaching very near to the MPP, rather keeps on oscillating or perturbing in both the directions around the maximum power point.

According to P&O algorithm at first step, the operating voltage of the PV panel is increased by a small incremental amount. If the resulting changes in power ΔP are positive, that means the power is increased, we keep on going or perturbing in the same direction by increasing the voltage. If power difference ΔP is negative, we are going away from the

direction of MPP and the sign of perturbation supplied has to be changed, means the voltage has to be reduced.
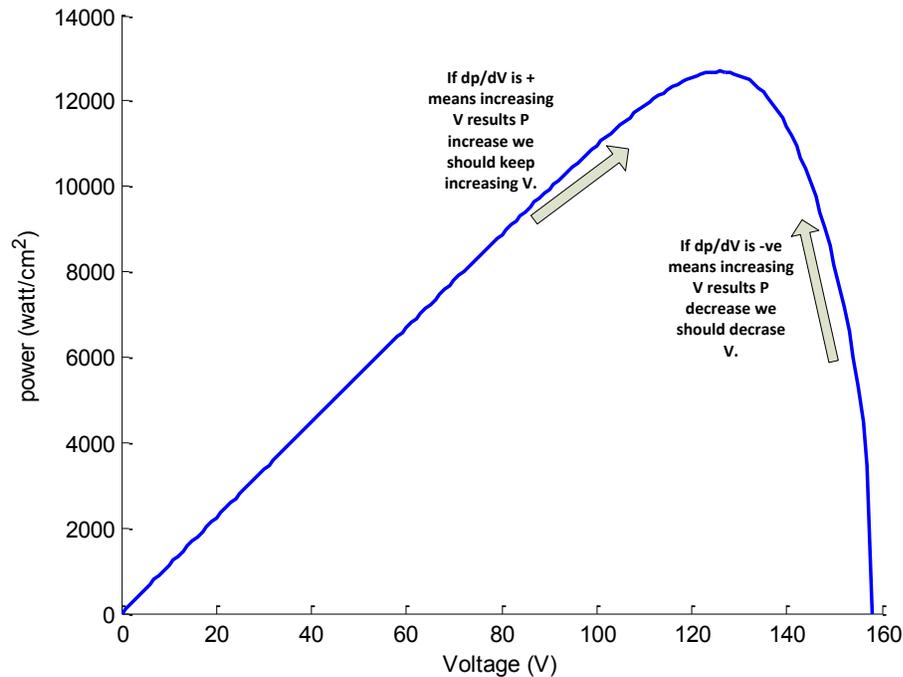
Figure 3.4: decision statement in P&O algorithm

Figure 3.4 shows the operation of the P&O technique using a plot of cell output power versus voltage for a solar panel. The Perturb and Observed algorithm operates by periodically perturbing the array terminal voltage or current and comparing the PV output power with that of the perturbation of the previous step in the cycle. The algorithm starts with a slight voltage perturbation introduced in the system that results the change in the power of the module. If the power increases due to perturbation then the perturbation is continued in that direction. When the power reaches to its maximum point, the power at the next perturbation decreases and hence after that the perturbation is reversed. In a

nutshell from the current voltage characteristics and power vs voltage curve of the solar cell the technique to reach MPP is,

At MPP $\dfrac{dP}{dV} = 0$

At left side of MPP $\dfrac{dP}{dV} > 0$;

At right side of MPP $\dfrac{dP}{dV} < 0$;

Therefore, taking D as a duty cycle of the dc-dc converter which is driven with the MPP algorithm we can say that, at MPP; $\dfrac{dP}{dV} = 0$, We keep D as it is means constant.

When left side of MPP; $\dfrac{dP}{dV} > 0$, We change D in such a way that V increases,

When right side of MPP; $\dfrac{dP}{dV} < 0$, We change D in such a way that V decreases

One of the problems could be with the P&O method that it could have slow dynamic response, when the value of the increment is small and low sampling rate is applied. But the low increment is necessary to decrease the steady state error and swing because the P&O always makes the operating point oscillate near the MPP. The smaller the increment, the lesser the swing and the closer the system will be to the array MPP. The bigger the increment, the faster the process or the algorithm will work, but the oscillation around the MPP point will be increased. For this a low increment is important to achieve a satisfactory steady state operation at MPP and the speed can be increased by increasing the sampling

rate. Therefore, there should always be a compromise between the increment and data reading (or the sampling rate) in the P&O MPP tracking.

The common problem in P&O algorithms is that the array terminal voltage and the power are perturbed every MPPT or sample cycle. So, when the Maximum power is reached, the output power swings or oscillates around the maximum point, resulting in power loss in the PV system by not operating always at MPP. This is especially true in slow varying atmospheric conditions like shading on PV cells.

As shown in Figure 3.4, the P&O algorithm operates by periodically perturbing the operating voltage and comparing it with the previous time step or instant. If both the power differences ΔP and the voltage difference ΔV between two successive instants are in the positive direction then there should be a small positive change in the array voltage. If either one of the voltage difference or the power difference is in the negative direction, then there should be a decrease in the array voltage. If both the array voltage and array power difference between two instants are in the negative direction then there should also be an increase in the array voltage. Similarly the next cycle should be repeated until the Maximum Power Point is tracked and reached.

The step by step methods in 'Perturb and Observe' are [18] :

1. Measure current, voltage and calculate power,

2. If the power is constant, return to measure the new values,

3. If power decreased or increased, measure the change in voltage,

4. According to the direction of voltage variation, modify the duty ratio.

The algorithm flowchart of the Maximum power point tracking is as follows
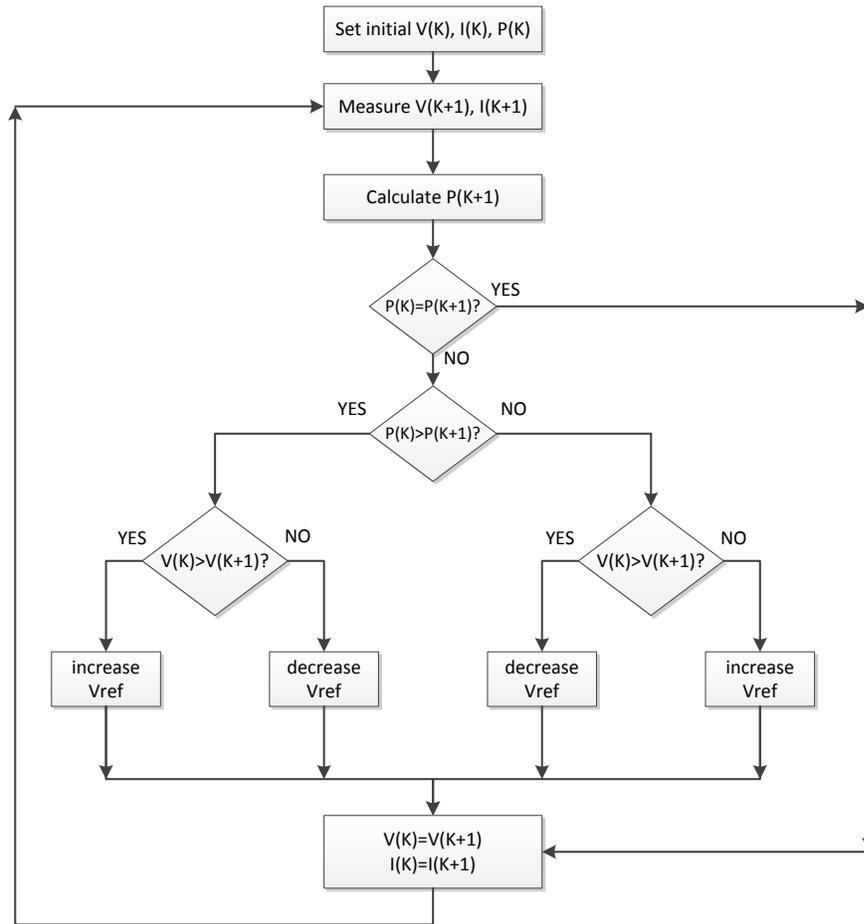
Figure 3.5: Perturb and Observe algorithm flowchart

The Simulink block of MPPT technique (P & O) is as follows
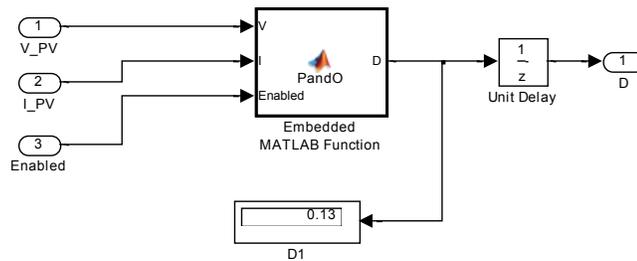
Figure 3.6: Simulink block diagram for MPP

3.4 Converter for MPP tracking
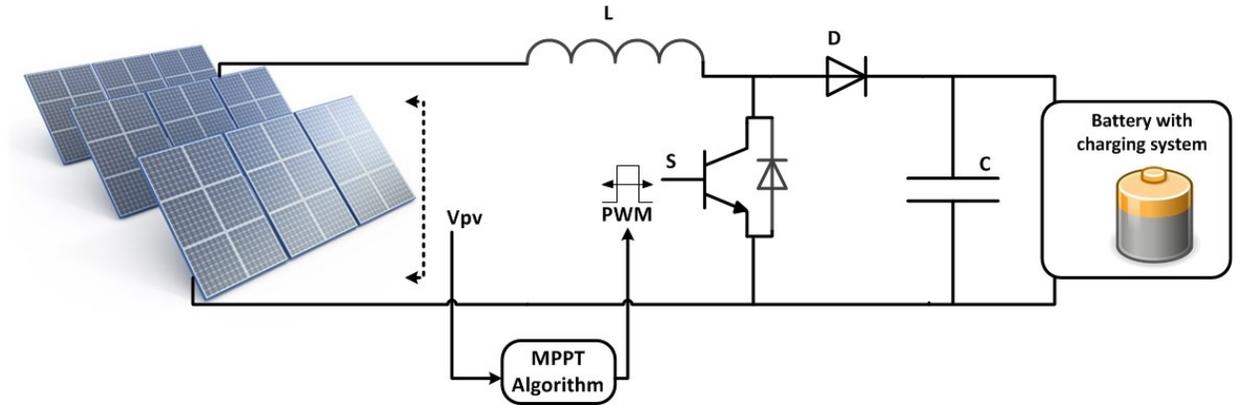
Figure 3.7: dc-dc boost Converter for MPPT

The Figure 3.7 shows that the PV array has been interfaced with the dc-dc boost converter using a controlled voltage source. The output from the PV array (the output voltage and current) is used to measure voltage and power difference between two samples of MPPT cycle and then to control the duty cycle by comparing the output signal from the MPP tracker with the saw-tooth waveform. This comparison generates the PWM signal which is fed as gate signal to the switch M.

3.5 Designing the dc-dc converter

We use DC-DC Converters as switching mode regulators to convert an unregulated dc voltage to a regulated dc output voltage. This voltage regulation is generally achieved by a PWM at a fixed frequency and IGBT or MOSFET is used as a switching device. By varying the duty cycle of the dc-dc converter we match input resistance of the panel since the Maximum Power Point Tracking is a load matching problem.
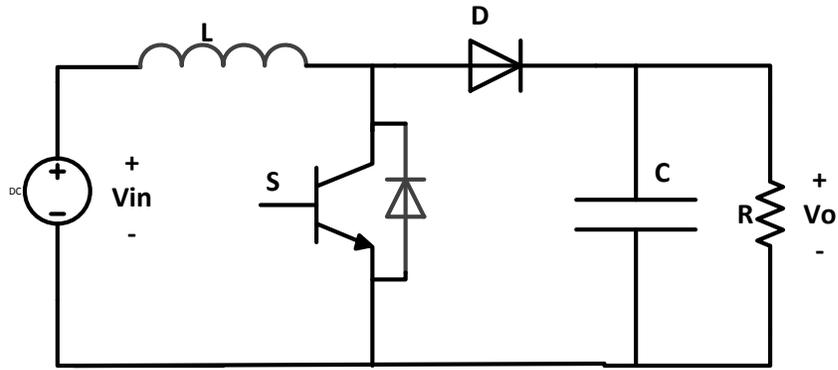
Figure 3.8: DC-DC Boost Converter

The dc-dc boost converter boosts the voltage to maintain the maximum output voltage constant for all the conditions of temperature and solar intensity variations. A simple dc-dc boost converter has been shown in Figure 3.8.

In steady state operation, the average voltage across the inductor over a full period is zero. In the boost converter like above the input voltage V_{in} and the output voltage V_o is related as,

$$V_{in} \times t_{on} - (V_o\text{-}V_{in}) \times t_{off} = 0$$
(3.1)

Where t_{on} and t_{off} is the on and off time of the switch. So if D is duty cycle of the dc-dc converter and T is the time period of the switching frequency we can write,

$$V_{in} \times D \times T = (V_o\text{-}V_{in} \times) \times (1\text{-}D) \times T \tag{3.2}$$

$$\Rightarrow V_o = \frac{V_{in}}{1-D}$$

$$\therefore V_{in} \propto (1\text{-}D) \tag{3.3}$$

As we used this DC-DC boost converter to track the maximum power point. D is the duty ratio of the dc-dc converter. We can see from equation (18) that if duty cycle

increases V_{in} decreases and if duty cycle decreases V_{in} increases. We control the duty ratio D of the converter in such a way that that the solar cell output voltage and current operates always at the maximum power point. The method is to apply a variation on the voltage (or on the current) towards bigger or smaller value, and to measure its impact appearing on the power value. If the power increases, the voltage should be changed (or the current) in the same direction, if not, the voltage should be changed in inverse direction as shown in the flowchart of Figure 3.5.

A boost regulator can step up the voltage without a transformer. The dc-dc boost converter that we use has high efficiency due to having a single switch. The input current is continuous as designed. The output voltage is very sensitive to changes in duty cycle D as we can see in equation (18). The average output current is less than the average inductor current by a factor of (1-D).

To operate the dc-dc boost converter in continuous conduction mode (CCM), the value of inductance L from the inductor current ripple analysis is given by equation (3.4) [27]

$$L_{min} = (1 - D)^2 \times D \times \frac{R}{2 \times f} \qquad (3.4)$$

A large filter capacitor is used to limit the output voltage ripples. The filter capacitor must provide the output dc current to the load when the diode D is revered biased or off.

The minimum value of filter capacitor that results in expected voltage swing ΔV_o across output voltage V_o is given by equation (3.5)

$$C_{min} = D \times \frac{V_o}{\Delta V_o \times R \times f} \tag{3.5}$$

We are using a 24 KW battery. So taking switching frequency 70 kHz we calculate L_{min} for our converter by applying equation (19),

$$L_{min} = (1 - D)^2 \times D \times \frac{R}{2 \times f} \text{ Or we can say,}$$

$$L_{min} = \frac{D \times V_{in} \times (1 - D)}{2 \times f \times I_{out}}$$

And $D_{min} = 1 - \frac{V_{imax}}{V_{omin}}$ and $D_{max} = 1 - \frac{V_{imin}}{V_{omax}}$

From current voltage characteristics from the solar cell we can see that V_{in} varies from 100 to 150 is good range to select MPP for any intensity. And also for the battery side Battery nominal voltage 300 and the battery full charge voltage is 350, 300 to 400 is a good range for converter output. But in that case there will not be good range for D to operate maximum power point. As converter output voltage is not important to us, to have a good range in duty cycle we will take input voltage from 10 to 360 voltage and output voltage 380 to 2000 voltages. Also with ripple current we consider inductor current 50 Amp. Therefore taking the values as,

$$V_{inmax} = 150, V_{inmin} = 100, V_{outmax} = 400 \text{ } and \text{ } V_{outmin} = 300$$

$$D_{min} = 1 - \frac{V_{inmax}}{V_{outmin}} = .05 \text{ and } D_{max} = 1 - \frac{V_{inmin}}{V_{outmax}} = .99$$

To calculate inductor value we need to consider all the possibilities.

For, $D = 1 - \frac{V_{inmax}}{V_{outmax}} = .82$

$$L = \frac{D \times V_{inmax} \times (1-D)}{2 \times f \times I_{out}} = \frac{.82 \times 360 \times (1-.82)}{2 \times 70000 \times 50} = 7.6\mu H$$

For, $D = 1 - \frac{V_{inmin}}{V_{outmin}} = .972$

$$L = \frac{D \times V_{inmax} \times (1-D)}{2 \times f \times I_{out}} = \frac{.82 \times 360 \times (1-.972)}{2 \times 70000 \times 50} = 1.4\mu H$$

For, $D_{min} = 1 - \frac{V_{inmax}}{V_{outmin}} = .05$

$$L = \frac{D_{min} \times V_{inmax} \times (1-D_{min})}{2 \times f \times I_{out}} = \frac{.82 \times 360 \times (1-.05)}{2 \times 70000 \times 50} = 2.44\mu H$$

For, $D_{max} = 1 - \frac{V_{inmax}}{V_{outmin}} = .99$

$$L = \frac{D_{min} \times V_{inmax} \times (1-D)}{2 \times f \times I_{out}} = \frac{.99 \times 360 \times (1-.99)}{2 \times 70000 \times 50} = .5\mu H$$

Taking 10% variation in the voltage that means $\frac{\Delta V_o}{V_o} = .1$, we can measure C_{min} by equation (20),

$$C_{min} = \frac{V_o}{\Delta V_o \times R \times f} = \frac{I_{out}}{\Delta V_o \times f} = \frac{50}{.1 \times 70000} = 7.14mF$$

So in our simulation, we took L=8μH and C=10mF. We took such a big value for the capacitor in order to establish large stable voltage to charge the battery.

Chapter 4: Battery basics and Charging System

4.1 Battery Basics

We need to address some definitions about battery and its charging system before going into details. This section also provides a basic knowledge, helps to understand the variables used to characterize battery operating conditions, and describes the manufacturer specifications used to understand and characterize battery's nominal and maximum parameters and values. A battery is a device that converts chemical energy into electrical energy and vice versa.

Some of the following basic battery definitions are taken from Ref [28] and Ref [29]

Cell, modules, and packs

A cell is the smallest, single entity packaged to form a battery can take and is generally has the voltage of the order of one to six. A module is consisted of several cells generally connected either in series or in parallel. In the same way, a battery pack is then assembled by connecting modules stack up together, again either in series or in parallel.

Battery types based on its chemistry

The most common types of battery chemistry can be classified as lead, nickel and lithium. Unfortunately, each system requires its own charging algorithm. Therefore, if provisions are made to change the charge setting, different battery charging system for different chemistries cannot be interchanged in the same charger. Also, not all batteries are created with equal characteristics or profile. Not even the batteries having the same

chemistry. The main trade-off in battery development is between power and energy. Batteries can be of either high-power or high-energy, but difficult to have both. Often manufacturers will classify batteries using these characteristics. There are other common characteristics to make classifications are like high durability, meaning that the profile has been changed in some way or other to provide higher battery life with the tradeoff of power and energy.

Secondary and Primary Cells

A primary battery is referred to the one that cannot be recharged. On the other hand a secondary battery is one that can be recharged.

Watts and Volt-amps (VA)

Power drawn from a battery is expressed in watts (W) or volt-amps (VA). Watt is the real power that is being metered; VA is the apparent power that determines the wiring size and the size of the circuit breakers. If the load is purely resistive the watt and VA readings are the same. A reactive load would introduce and cause a drop in the power factor (PF) from the ideal value that is 1 to a lower value like 0.8, 0.7 and so on.

C-rates

A C-rate is a measure of the rate at which a battery is discharged or charged relative to its maximum capacity. C-rates specify charge and discharge currents. A 1C rate means the battery discharges entirely in one hour at a current marked with Ah rating. Similarly theoretically the battery could be charged to its full capacity in one hour with a charging current specified in Ah rating. For a battery with a capacity of 50 Amp-hrs., if the battery

discharges in 1C rate, it will take 50 amps to discharge the battery in 1 hour. In 2C rate for this discharge current would be 100 Amps and it would be discharged in 30 minutes. And a C/2 rate would be 25 Amps and will be discharged in 2 hours. Similarly, an E-rate describes the discharge power. A 1E rate is the charging or discharging power to charge or discharge the entire battery in 1 hour. So we can say that on charge, 1C charging rate takes a good battery to charge in about 1 hour; 0.5C takes 2 hours and 0.1C charging arte would take 10 to 14 hours. In describing batteries, discharge current is often expressed as a C-rate in order to normalize against battery capacity that varies from batteries to batteries, manufacture to manufacture and chemistry to chemistry.

The battery capacity meaning the amount of energy a battery can contain can be measured with a battery analyzer. This battery analyzer or the measuring device discharges the battery at a certain calibrated current while measuring the time it takes to reach the end-of-discharge voltage. If the discharge at a rate of its Ah current lasts for 15 minutes before reaching the end of discharge cutoff voltage, then the battery has a capacity of 25% of its rated capacity. If it lasts for 30 minutes, the capacity is 50% of rated capacity. When discharging a battery with a battery analyzer capable of applying different C-rates, a higher C-rate will produce a lower capacity reading and vice versa. By discharging the 1Ah battery at a charging rate of 2C means 2A the battery should ideally deliver the full capacity in 30 minutes [28].

Battery Capacity

Capacity represents the specific energy in ampere-hours (Ah). It is the total Amp-hours available when the battery is discharged at a certain discharge current specified as a

C-rate from 100 percent state-of-charge to the state of charge acquired at the cutoff voltage. Capacity is calculated by multiplying the discharge current (in Amps) by the discharge time (in hours). Clearly it is understandable that it decreases with increasing C rate. One can use a battery for different Ah requirement than that of the Ah mentioned in the battery specifications but with correct voltage, provided the rating Ah mentioned is high enough because in that case the discharging would not damage the low rate charging chemistry profiled battery. Chargers have some tolerance to batteries with a range of some Ah ratings. A larger capacity battery will take longer to charge than a small one.

Energy

The energy or the "energy capacity" of the battery is the total Watt-hours available when the battery is discharged at a certain discharge current specified as a C-rate from full 100 percent state-of-charge to the state of charge acquired at the cutoff voltage. Energy is calculated by multiplication of the discharge power in Watts and the discharge time in hours as in this case of energy discharge power is used instead of discharge current as in the case of capacity. Same as capacity, energy decreases with increasing C-rate.

Battery Voltage

The voltage mentioned on the body or specification of the battery refers to the nominal battery voltage. It is the reported or reference voltage of the battery, also sometimes thought of as the "normal" voltage of the battery. A load or a charger associated to a voltage, differed than the nominal voltage, should not connect to the battery.

The voltage between the battery terminals with no load applied. The open-circuit voltage depends on the battery state of charge, increases with state of charge. The open

circuit voltage (OCV) on a fully charged battery can be slightly higher than the nominal voltage.

And the closed circuit voltage (CCV) represents the battery voltage under load or on charge and the readings will vary accordingly. It sometimes is referred as terminal voltage. It varies with SOC and discharge/charge current.

The minimum allowable voltage is called Cut-off Voltage. It is this voltage that generally defines the "empty" state of the battery.

State of Charge (SOC) (%)

State of charge or in short SOC is an expression of the current battery capacity at a time as a percentage of maximum capacity. It is calculated by current integration to determine the change in battery capacity over time. It varies between 0 and 100%. The SOC for a fully charged battery is 100% and for an empty battery is 0%. The SOC is calculated as:

$$SOC = 100\left(1 - \frac{1}{Q}\int_0^t i(t)dt\right)$$

Depth of Discharge (DOD) (%)

The percentage of battery capacity that has been discharged expressed as a percentage of maximum capacity. A discharge to at least 80% DOD is referred to as a deep discharge.

Specific Energy (Wh/kg)

Specific energy is the battery energy or nominal battery energy per unit mass. Specific energy is a characteristic of the battery chemistry and packaging. It determines the battery weight required to achieve a given energy range in case of electric vehicle, along with the energy consumption of the vehicle.

Specific Power (W/kg)

Specific power is the maximum available power per unit mass. It is also a characteristic of the battery chemistry and packaging. It determines the battery weight required to achieve a given performance target.

Maximum Continuous Discharge Current

It is the maximum current at which the battery can be continuously discharged. The limit is usually defined by the battery manufacturer in order to prevent excessive discharge rates that would damage the battery or reduce its capacity. In case of electric vehicle this parameter is important, because this defines the top sustainable speed and acceleration of the vehicle as it is associated with the maximum continuous power of the motor of the vehicle.

Charge Voltage

Charge voltage is the voltage that is used to charge the battery when being charged to its full capacity. Charging schemes generally consist of a constant current charging until the battery voltage reach to its charge voltage or the predefined value of the voltage at which the constant voltage charging start charging allowing the charge current to taper until it is very small.

Float Voltage

It is the voltage at which the battery is maintained after being charge to 100 percent SOC to maintain that capacity by compensating for self-discharge of the battery.

Charge Current

Charge current is the ideal current at which the battery is initially charged (to roughly 70 percent SOC) under constant current charging scheme before transitioning into constant voltage charging.

4.2 Basic Charging Methods

4.2.1 Constant Voltage charging

The method in constant voltage charging is to keep the voltage constant across the battery terminal all the times not considering the SOC or other battery conditions. A simple form can be a DC power supply consists of a step down transformer with a rectifier. These types of techniques are used in the lead acid batteries that are being used in cars and backup power systems and typically use constant voltage chargers. In addition, Li-ion (lithium-ion) cells often use constant voltage systems, although these charging systems are usually more complex with added circuitry to protect both the batteries and the user safety.

It is worth of mentioning that constant voltage charge provides high initial current to the battery and charger. As the battery charges, its voltage increases. This causes a corresponding rapid decrease in charging current as depicted in the Fig. 4.2.
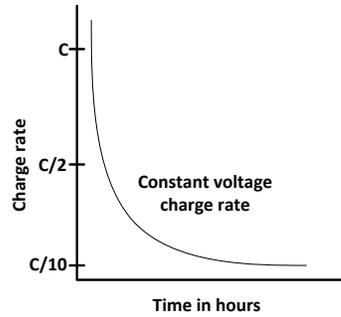
Figure 4.1: Charging rate VS time in Constant Voltage Charging [29]

As a result even though battery reaches to partial charge quickly, obtaining a full charge requires long time. These chargers are frequently found in the applications that normally allow extended charging periods to attain full charge.

Constant voltage charging method is mostly used from two different viewpoints. It is used as a fast charger to restore a high percentage of charge in a short time. And secondly and most importantly it is used as a float charger to minimize the effects of overcharge on batteries having infrequent discharges.

4.2.2 Constant current charging

Constant current chargers vary the voltage they apply to the battery to maintain a constant current flow and injecting constant current or injecting at a lower rate when the voltage reaches the level of a full charge. In this method a uniform current is driven through the battery in an opposite direction of discharge. This is in fact pushing the charges, as the flow of charges is current, at a constant rate no matter how full the battery with charge is. There is a major drawback to this approach. The battery is always being pushed at a

constant rate. So, when it is close to being fully charged, if the charger would force extra current into the battery, it could cause overcharging. The ability to bypass or slow down this current is very important to a good charging method. With monitoring the voltage on the battery or by end of charge detection method, the charging level can be determined. When it is determined at a certain point, the current source would need to be folded back to only maintain a trickle charge and prevent overcharging.

It is important to note that there is a term called pulsed chargers feed the charge current to the battery in pulses. The average current is considered as charging rate and this can be precisely controlled by varying the width of the pulses. During the charging process, short rest periods of few milliseconds, between pulses would allow the chemical actions to pass on through the bulk of the electrode before recommencing the charge. In this way, it allows the chemical reaction to keep pace with the rate of inputting the electrical energy [30] [31]. It is also claimed that this method can reduce unwanted chemical reactions at the electrode surface such as crystal growth and passivation and gas formation etc.

4.2.3 Multi-stage Charging

Multi stage charging used in this thesis involves the advantages of both constant voltage and constant current charging. Charging algorithm developed here combines the two methods to achieve less charging time as possible, with no or minimum damage to the charging cell. It has CC (Constant Current) Mode where the system tries to maintain C/2 charging rate based on some conditions defined in the algorithm. The charging mode changes from (CC) Constant Current to CV (Constant Voltage) mode based on the alternate

conditions and when the battery is charged about to its full capacity. With this Switching Point between CC and CV the battery charger can adjust the current automatically according to the battery capacity. Near to the full charge the charger maintains a constant battery voltage and the current slows down. Charger is supposed to be left connected without harming the battery. If the battery voltage and the capacity drop to a certain level, the charger changes from any mode to Constant Current mode and restart charging.

4.3 Charging Rates

A very simplest Charging algorithm is proposed to validate the charging capability of our solar source by simulation. The circuitry to recharge the batteries in a portable product is an important part of any power supply design. The complexity (and cost) of the charging system is primarily dependent on the type of battery and the recharge time.

Before discuss about the algorithm we need to know charging methods, end-of-charge-detection techniques, and charger circuits for use with Nickel-Cadmium (Ni-Cd), Nickel Metal-Hydride (Ni-MH), and Lithium-Ion (Li-Ion) batteries.

Batteries can be charged at different rates depending on the requirement. Typical rates are described below [31].

- Slow Charge = Overnight or 14-16 hours charging at 0.1C rate

- Quick Charge = 3 to 6 Hours charging at 0.3C rate

- Fast Charge = Less than 1 hour charging at 1.0C rate

4.3.1 Slow Charge

Slow charge is usually defined as a fixed charging current of about c/10 (1/10 of the cell's A-hr. rating) that can be applied to the battery indefinitely without damaging the cell. Trickle charging is another name of this method. They are very simple and have no full-charge detection. The charging time in this type of charging on an empty battery is 14 to 16 hours as mentioned earlier. When the cell is fully charged, continued charging may cause to form gas within the cell. So, all of the gas formed must be able to somehow suppressed or recombine internally, otherwise pressure built up within the cell eventually leads to release gas through opening of the internal vent which may reduce the life of the cell. Therefore, the maximum safe trickle charge rate is not only dependent on the chemistry but also on the construction of the electrodes.

The big advantage of slow charging is that theoretically it uses the charge rate that requires no end-of-charge detection circuitry, since it cannot damage the battery regardless of how long it is used. This means the charger is simple and very cheap. But we need to remind that in case of smaller battery the continuous current may hit up the pack. And as there is no provision to terminate the charge, heat built up shortens the life of the pack. On the other hand in case of bulk battery, the battery may never reach full charge and remains cold. As the battery does not receive a full charge, performance could be poor. If the chemistry is nickel based, undercharged would gradually cause to lose the ability to accept a full charge because of crystalline formation. Another big disadvantage of slow charge is that it takes a long time to recharge the battery.

The ability to easily charge a Ni-Cd battery in less than 6 hours without any end of charge detection method is the primary reason; they dominate cheap consumer products like toys, flashlights, soldering irons etc. It is even claimed that some high-rate Ni-Cd cells can tolerate trickle charge currents as high as c/3.

Ni-MH cells are not as tolerant of continuous charging. The maximum safe trickle charge rate in case Ni-MH is somewhere between c/40 and c/10 [32]. If continuous charging is to be used with Ni-MH without end of charge detection process, care must be taken not to exceed the maximum specified trickle charge rate, if not it would be damaged.

Lithium ion cells however cannot tolerate overcharging or overvoltage and the charge should be terminated immediately when the upper voltage limit is reached. Therefore, in our algorithm immediate charge termination option has been provided as it is designed for Li-ion. Smart Chargers servicing a broader range of batteries need some intelligence to supervise the charging scheme and should have ability to control the current when full and provide safety if any disasters happens. Especially for Li-ion battery efficient scheme for recharging could be an important issue [33] [34].

4.3.2 Rapid/Quick Charge

The rapid/quick charger falls between the slow and fast chargers and charges the battery in 3 to 6 hours with charging rate of 0.3C. It is better suited to service nickel and lithium based batteries. If not specially designed, the rapid charger cannot service both nickel and lithium based chemistries. Most rapid chargers include temperature protection to safeguard against failures. Because increasing charging rate may cause to increase the possibilities of overcharging or overheating. When the battery is reached to its full charge,

preventing the battery from overheating and terminating the charge, is not simple. Different types of chemistry have different types of charging curves and battery chargers must be designed to detect the end of charge detections for the specific chemistry involved. In addition, some form of Temperature Cut off, in short TCO technique or Thermal Fuse must be used to prevent the battery from overcharging hence overheating.

These features offer improved service over the slow charger and batteries but they are more complex and expensive to build. Also, since these chargers are designed for specific chemistries, it is not normally possible to charge one cell type that was designed for other. But as mentioned above, universal chargers are able to charge all cell types. They have sensing devices to identify the cell type and apply the appropriate charging profile.

For electric vehicle, charging time may seem longer comparing to energize a regular vehicle. Assuming no efficiency loss in the charger, a 10 Hour 3 kW charger will put 30 kWh of energy into the battery which is enough for about 100 miles. Comparing to that, a regular car would take about 3 minutes to put enough chemical energy into the tank to provide 90 kWh of mechanical energy which is sufficient to take the car 300 miles.

4.3.3 Fast Charge

Fast charge is usually defined as a 1 hour charging time, which is associated to a charging rate of 1 to 1.2 C rate. The larger power supply and more complex control circuits reserve fast chargers mostly for commercial use, such as medical, military, communications and power tools. It needs tighter communication between the charger and battery. At a 1C charge rate, fast charger needs a little more than an hour to charge an

empty Ni-Cd and NiMH battery. The difference in chemical reactions occurring within the Ni-Cd and Ni-MH battery during charge is endothermic meaning cell get cooler in case of Ni-Cd and exothermic meaning cell heated up in case of Ni-MH. That makes possible to safely force very high rates of charging current into a Ni-Cd cell, as long as it is not overcharged. Only the internal resistance limits the maximum safe charging current for Ni-Cd and causes power dissipated as $P = I^2R$. The internal impedance is usually quite low for Ni-Cd; hence high charge rates are possible. High rating Ni-Cd cells can tolerate charge rates of up to 5c. On the other hand in case of Ni-MH the exothermic nature limits the maximum charging current that can be safely used. As a battery approaches full charge, some nickel-based chargers reduce the charge current and when the battery is full the charger switches to trickle charge or maintenance charge.

Most nickel-based fast chargers accommodate Ni-Cd and NiMH batteries on the same algorithm, but not Li-ion. To service Li-ion based chemistries in the same charger, a provision is needed to select the correct charging algorithm. Usually, Li-ion batteries are easier to charge than Ni-Cd and NiMH. The charge to 70 percent at 1C occurs in less than an hour, the rest of the time is devoted to trickle charge.

Lead acid batteries cannot be fast-charged. Most lead acid chargers charge the battery in 14 hours and anything slower may be a compromise. As comparing to all chemistries, lead acid can be charged relatively quickly to 70 percent and the important saturation charge takes up the remaining time. Partial charge at high rate provides the battery receiving a fully saturated charge once every few weeks to prevent sulfation [28].

So based on charging chemistry we can associated different algorithms to different charging chemistry.

Type	Chemistry	C-rate	Time	Temperatures	Charge termination
Slow charger	NiCd Lead acid	0.1C	14h	0ºC to 45ºC (32ºF to 113ºF)	Continuous low charge or fixed timer. Subject to overcharge. Remove battery when charged.
Rapid charger	NiCd, NiMH, Li-ion	0.3-0.5C	3-6h	10ºC to 45ºC (50ºF to 113ºF)	Senses battery by voltage, current, temperature and time-out timer.
Fast charger	NiCd, NiMH, Li-ion	1C	1h+	10ºC to 45ºC (50ºF to 113ºF)	Same as a rapid charger with faster service.
Ultra-fast charger	Li-ion, NiCd, NiMH	1-10C	10-60 minutes	10ºC to 45ºC (50ºF to 113ºF)	Applies ultra-fast charge to 70% SOC; limited to specialty batteries.

Table 4.1: Each chemistry uses a unique profile and charge termination [28]

4.4 End-of-charge detection

Ni-Cd and Ni-MH batteries can be fast charged safely just making sure not to over-charge. Various methods can be used to determine full charge. To detect the full charge point correctly, voltage or temperature is typically the primary method, alongside a timer, in case the backup fails. Temperature sensing is preferable to voltage sensing because the cell temperature gives the most accurate information about what is happening within the cell. However, to measure the cell temperature accurately, the temperature sensor must be built inside the battery pack which increases the manufactured cost of the battery. Therefore, voltage sensing is easier, as voltage leads are easily reachable from outside and require no special assembly inside battery pack.

4.4.1 Temperature Detection Methods

There is no significant increase in the temperature in Ni-Cd cell until nearing full charge, as the charging process is endothermic means cell gets slightly cooler during charging. But when the full charge is reached, the amount of energy used in the endothermic reaction decreases and this amount dissipates as heat making the cell get hot. On the other hand temperature in the Ni-MH cell increases all the time during charging, as it is exothermic.

ΔT Detection

As the full charge is reached, the rate of the temperature increases very sharply. Almost all the cells temperature rise of about 10°C above ambient when the cell is fully charged assuming a 1c charge rate. So, circuit which can cut off the high current charge at this 10°C rise point can be used with either battery types. This circuit is called a ΔT detector.

Temperature slope detection

During fast charge, the temperature of both Ni-Cd and Ni-MH cells starts increasing very rapidly when full charge is reached. A circuit which measures the rate-of-change (slope) of the cell temperature can be used for end-of-charge detection with both Ni-Cd and Ni-MH batteries.

4.4.2 Voltage Detection Methods

The voltage during fast charge can be used to determine when it is fully charged not by the magnitude, but by the rate of voltage change. The two techniques discussed in this paper are ΔV and Slope Detection.

ΔV Detection

The drop in battery voltage is used to terminate fast charge in a -ΔV Detection, which continuously monitors the battery voltage and shuts off the charger when the voltage drops by a preset amount. The voltage of the Ni-Cd single cell used to drop 45 mV when the cell temperature was 10°C above ambient. As discussed in previous section, a 10°C rise is typically used as the full charge cutoff for a Ni-Cd cell that is charged at 1c. Battery makers typically recommend a -ΔV detection threshold of 10-20 mV/cell in charging systems that are dedicated to Ni-Cd only. The Ni-MH cell also exhibits a dip in voltage, but it is much smaller which could be typically few mV [32].

Voltage Slope Detection

A microprocessor based system that have the ability to measure, store and compare battery voltage readings taken at sampled intervals can accurately detect end-of-charge by using a method called voltage slope detection. The detection system would identify zero slope when two successive voltage readings were the same over a timed interval.

4.5 End of charge of detection in simulation

As the main concern of our simulation is the application of the modeled solar cell in battery charging we used the direct state of charge detection parameter in our simulation that the Simulink battery block provided us. The mathematical representation of SOC as mentioned in the previous chapter also is

$$SOC = 100\left(1 - \frac{1}{Q}\int_0^t i(t)dt\right)$$

$$(4.1)$$

Chapter 5: Charging algorithm and implementing charging circuit

5.1 Introduction

In many cases, the battery-charging system is given low priority, especially in cost-sensitive applications. The quality of the charging system plays a key role in the life and reliability of the battery. Developing an optimized charging system for Nickel-metal-hydride (NiMH) and lithium-ion (Li-ion) batteries, familiarity with the fundamental

requirements for charging these batteries is essential. During implementation one should be aware of the tradeoffs of linear versus switch-mode charging solutions. One of the important functions of a charge controller in a stand-alone PV system is to protect the battery from overcharge and over discharge. Any system having unpredictable or swinging loads, user intervention, optimized or undersized battery storage (to minimize initial cost) or other characteristics that would allow excessive battery overcharging or over discharging requires a charge controller [35][36].

5.2 Advantages and disadvantages of different charging methods

Before describing battery charging system let us briefly explain some advantages and disadvantages of constant current and constant voltage charging system in points from referred from section 4.2.

5.2.1 Advantages of Constant Voltage charging

- This is the simplest form of charger. So the circuitry for this type charger is simple. A DC power supply consists of a step down transformer with a rectifier can be enough to provide the DC voltage to charge the battery. This type of simple designs is often found in cheap car battery chargers.

- The constant voltage charge provides high initial current to the battery and charger. So, battery reaches to partial charge quickly. Constant Voltage chargers are frequently found in the applications that normally allow extended charging periods to attain full charge.

- The most importantly it is used as a float charger to minimize the effects of overcharge on batteries having infrequent discharges.

- In case of charging a battery with solar cells which is in fact our case, though it provides a constant current it is dependent on light intensity and other uncontrollable variability in the environment. So in this case constant voltage charge seems to fit well which does not depend on the current provided by the source. So, this method may eliminate the dependence of the charger on external variations like the time of day, weather conditions or temperature.

- Entirely constant voltage charging often does not need the end of charge detection circuitry. So, it is possible sometimes to avoid end of charge detection circuit of constant voltage charging. That is why cheap charger generally uses this method without end of charge detection circuit.

5.2.2 Disadvantages of Constant Voltage charging

- As the battery charges, its voltage increases. As a result even though battery reaches to partial charge quickly, obtaining a full charge requires long time.

- This method is better not to use where frequent cycling of the battery is necessary. Repeated discharges without returning the cell to its full charge will eventually decrease the battery capacity and may damage individual cells.

5.2.3 Advantages of Constant Current charging

- If the constant current can be pushed to a battery at the pace of its chemical reaction, the overall charging time to reach its full capacity takes less time than the other method.

- It is also claimed that this method can reduce unwanted chemical reactions at the electrode surface such as crystal growth and passivation and gas formation etc.

5.2.4 Disadvantages of Constant Voltage charging

- The battery is always being pushed at a constant rate. So, when it is close to being fully charged, if the charger would force extra current into the battery, it could cause overcharging.

- As for constant current charging it is important determine end of charge detection to stop or to detect over charging. So, to introduced the end of charging method in the additional circuitry is required and this makes the whole circuit complex.

5.3 Battery Charging System

Solar batteries provide energy storage in renewable energy systems and are cycled, on a daily basis. In battery charging system we include SOC, nominal voltage and charging current to determine when to switch between current and voltage mode and when to cut the source or the load. Battery state of charge (SOC) is the cumulative sum of the daily charge/discharge energy transfers [31]. It can be seen that the daily energy demand is approximately constant. Smart system should include SOC in battery charging [37]. However as the two control algorithms (MPP and battery charging) are working in the

same system, mismatch between PV system and battery bank might have been happened [16]. One should be aware of these types of mismatches during system implementation. Constant-current / Constant-voltage (CC/CV) controlled charge system is used for charging NiMH, Li-ion and some other batteries where damage is more probable if the upper voltage limit is exceeded.

When Fast Charging rates are specified, they are usually referred to the constant current or CC mode. Depending on the cell chemistry this period could be between 60% and 80% of the time to charge fully. There is a major drawback to this approach. Since the battery is always being pushed at a constant rate, when it is close to full charge, the charger could force extra current into the battery, causing overcharge. For this reason it is recommended that the charging method switches to constant voltage before the cell voltage reaches its upper limit. This implies that chargers for Lithium Ion cells must be capable of controlling both the charging current and the battery voltage. Before going to charging algorithm it is worth mentioning about smart battery concept that has interchangeable charging profile. The idea of interchangeable referred to exchanging the original battery with one that had the same voltage range. There are several issues to deal with it. Also it is to be noted that Nickel metal hydride charging and the end of charge termination or detection is much simpler than lithium ion battery charging. Lithium Ion has Intra-chemistry issues and it comes in many different types varying from manufacturer to manufacturer [38]. To face the challenges of those issues, smart battery concept is also described in this thesis.

5.4 Charging algorithm

Based on the discussion in the previous chapters and considering the precautions and challenges mentioned in the previous section to develop a charging algorithm with multistage mode of Constant-current and Constant-voltage (CC/CV) for a 24KW Li-ion battery, we address the following points:

1. We used both constant voltage and constant current charging. The charging system starts with constant current charging and switch to constant voltage charging in a point based on the understanding of the battery chemistry and the specifications on which the constant voltage charging would provide the battery the safe charging environment.

2. We need to consider that, since the battery is always being pushed at a constant rate as mentioned in the battery charging methods section when it is close to being fully charged, the charger would force extra current into the battery, causing overcharge. The system should have the ability to bypass or slow down this current which is the key to a successful charger.

3. As also mentioned in the previous sections by monitoring the voltage on the battery, the charging level can be determined. And at that point, the current source must need to be folded back to only maintain a trickle charge and prevent overcharging. Therefore, at that point we should switch to constant voltage from constant current charging.

4. Now the point of switching we defined here is based on state of charge. It can also be fixed to a certain voltage value. In our simulation process when voltage reaches at

certain SOC point we take the voltage at that point and keep the charging to that constant voltage.

5. However, the constant voltage method is better to use where frequent cycling of the battery is necessary. Because repeated discharges without returning the cell to its full charge will eventually decrease the battery capacity and may damage individual cells. Therefore, we need to be careful about switching point between constant current to constant voltage.

6. Constant voltage is used as a float charger to minimize the effects of overcharge on batteries having infrequent discharges. Therefore, considering the point 5 we should keep in mind that during selecting the voltage it should not be very high that it would aid the overcharge and also at the same time should not be small that the battery would not reach to its almost full charge frequently.
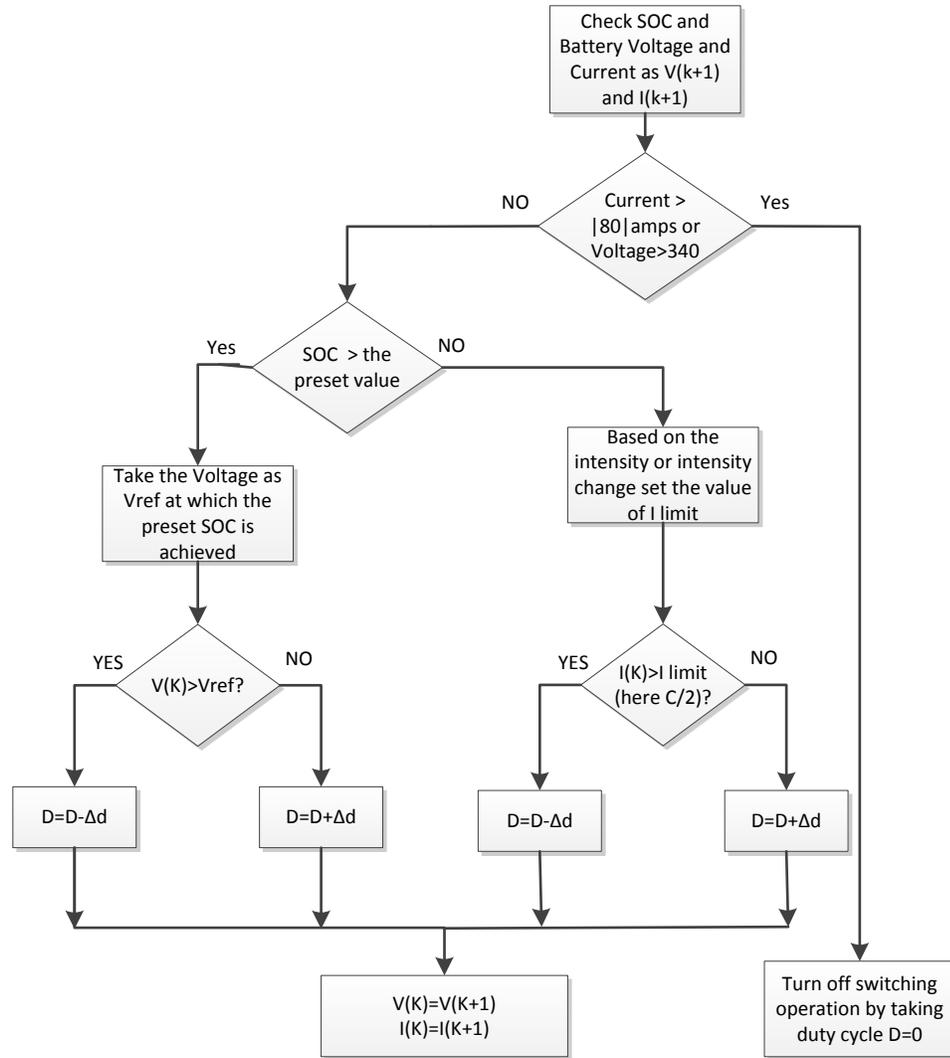
Figure 5.1: Battery charging algorithm with over charge and over discharge protection

The charging algorithm works well for the second generation solar cells without affecting the MPP algorithm. Furthermore in case of including multi-level current charging provision could be provided to shift the current at different level when the shading shifts the MPP to different point and if the current used for charging is not desired enough, it would switch between CC and CV whenever needed.

5.5 Charging converter

For the charging the battery we used two quadrant dc-dc converter. The switching network of Maximum power point tracking is employed with single quadrant switch. Each semiconductor element is able to conduct current of only one polarity in the on state, and block voltage of one polarity in the off state. This suggests that, for proper functioning of the switch network, the source voltage, load voltage, and inductor current must all be positive. Consequently, the network allows the instantaneous power to flow in one direction only: from the source towards to load. But for battery charging, bidirectional (regenerative) power flow is obtained with a current-bidirectional two quadrant realization of the switch network [39].
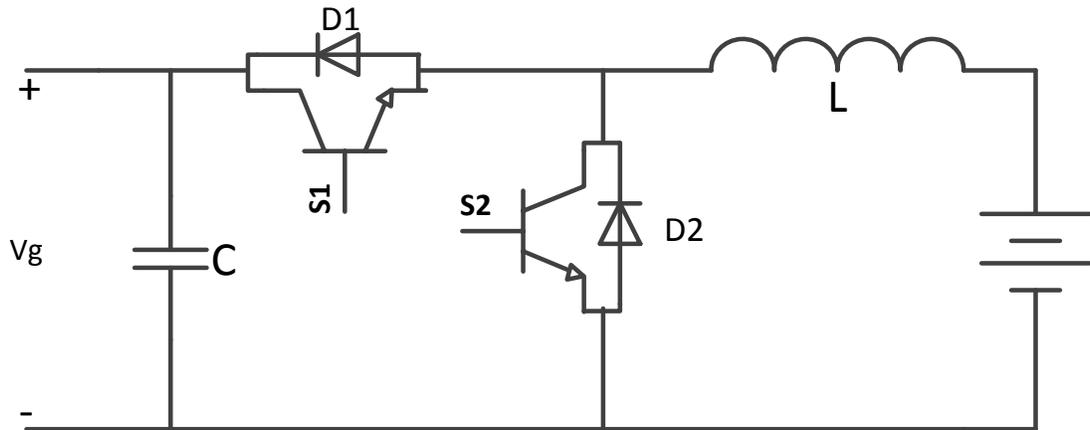

Figure 5.2: DC-DC Buck converter with two-quadrant switches capable of bidirectional power flow

An example is illustrated in Figure 5.2, in which a dc-dc buck converter is interfaced with the batteries. The anti-parallel-connected transistors and diodes form the

current-bidirectional switches. IGBT S2 is driven with the complement of the S1 drive signal, such that S2 is off when S1 is on, and vice-versa.

To charge the battery, the inductor current $I_L(t)$ is positive and flows through switch S1 and diode D2. During discharging of the battery, the current $I_L(t)$ reverses polarity, and flows through switch S2 and diode D1. The magnitude and polarity of the battery current can be controlled via adjustment of the duty cycle D. Switching loss imposes an upper limit on the switching frequencies of practical dc-dc converters.

Several mechanisms lead to switching loss. The diode reverse recovery process induces substantial additional energy loss in the switch during turn-on period. The energy stored in the semiconductor output capacitances is dissipated during the switch turn-on period. Energy stored in leakage inductances and other stray inductances is usually dissipated by the transistor during the turnoff period. The total switching loss is equal to the sum of the energy losses that arise by these inductances, multiplied by the switching frequency [39]. A large inductor value is used in this converter to push the 40 amp current as well as to prevent the spike and or large ripple. It also prevents the battery from over discharge before detecting any large discharge current. Because, instead of an output capacitor in a conventional converter we have a very large vehicle standard battery and if we calculate the equivalent capacitance of the battery and we get

$$\frac{1}{2}cv_2{}^2 = 24KWh => C = \frac{2 \times 24000 \times 3600}{350^2} = 1410F,$$ it is a huge capacitance value, compared to any conventional capacitor.

Therefore, to design the inductor for buck convertor by using following equation taking the frequency as 1kHz and ripple current 1 amp we get,

$$L = (V_{in,max} - V_{out}) \times \frac{V_{out}}{V_{in,max} \times freq \times I_{ripple}}$$

$$= (2000\text{-}350) \times \frac{350}{2000 \times 1000} = .3\text{H}$$

The inductor is used near the battery for several purposes. We used DC-DC buck converter. And for the conventional two quadrants DC-DC buck converter the inductor is near capacitor or load. It gives stable constant current to the battery and large value of it is also being used to transfer the stored energy to the large capacitor equivalent to the battery that we just calculated.

Chapter 6: Results and Discussions

6.1 Introduction

The J-V characteristics for asingle solar cell for different intensities are shown in Figure 6.1. The parameters for the J-V characteristics are given in Table 6.1.

Parameter	Value
λ (nm)	300 to 900 nm
W (cm)	1.8×10^{-4}
d (cm)	$.2 \times 10^{-4}$
T(K)	300
τ'_h (s)	$.2 \times 10^{-6}$
τ'_e (s)	$.1 \times 10^{-6}$
μ_h (cm^2/V/s)	5
μ_e (cm^2/V/s)	180
n_i (cm^{-3})	2.23×10^6
A	1.8
V_{bi} (V)	1.1
V_0 (V)	.8
R_s(Ωcm^2)	6

Table 6.1: parameters and their values for CdS/CdTe

**6.2 Verification with experimental data**
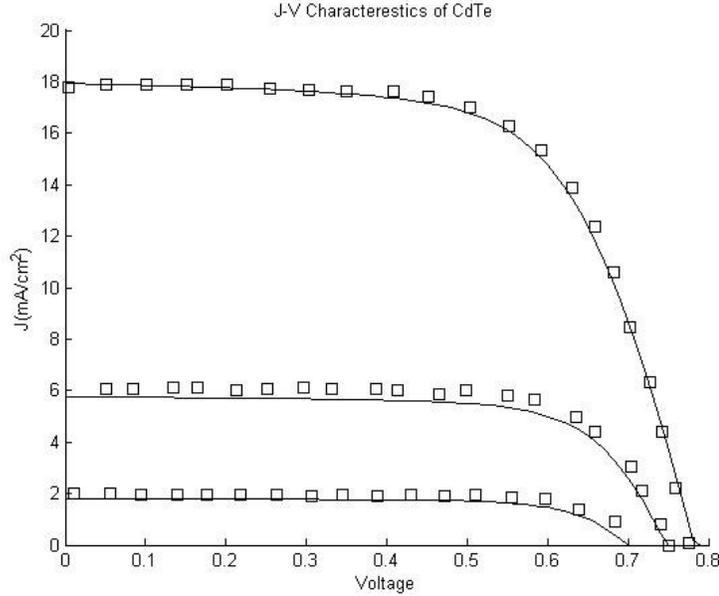
Figure 6.1: Current Voltage characteristics with experimental data

The J-V characteristics of a CdS/CdTe solar cell at different sun intensities (100, 32, and 10% sun intensities at AM 1.5) are shown in Figure 6.1. The solid lines represent the proposed modeled curve and the symbols represent experimental data and. Ref [21] provides all the experimented data were taken from. The CdTe thickness is taken as 2 μm. The CdS thickness is as 0.2 μm. The theoretical models are almost fit with the experimental data. The best values for $\mu\tau'$ of holes and electrons are $\mu_h\tau_h' \approx 10^{-6}$ cm²/V and $\mu_e\tau_e' \approx 5.4 \times 10^{-5}$ cm²/V, which are consistent with the $\mu\tau'$ values for CdTe [40] [41] . Assuming typical values for electrodeposited CdTe layer, $\mu_h = 5$ cm²/V-s [41] and $\mu_e = 180$ cm²/V-s the carrier lifetimes become, τ_h'=0.2 μs and $\tau_e' = 0.3$ μs. The other fitted parameters in for the model could be Figure 6.1 are $V_0 = 0.8$ V, $A = 1.8$, $R_s = 6\Omega$-cm², and $R = 0.25$ [19].

The diode quality factor is 1.8, which suggests that the recombination current is more significant than the diffusion current.

6.3 Current voltage characteristics of PV array

By arranging the no of cells into series and parallel as defined in section 3.1 before in modeling of PV array we took 200 series and 200 parallel cells. In that case the series resistance is 6 ohm. The general equation for series resistance when developing a PV array is

$$R_{array} = \frac{no.\,of\ series\ cells}{no.\,of\ parrallel\ cells} \times R_s \qquad (6.1)$$

Thus, for 200 series and 200 parallel cells, the series resistance = 6 ohm
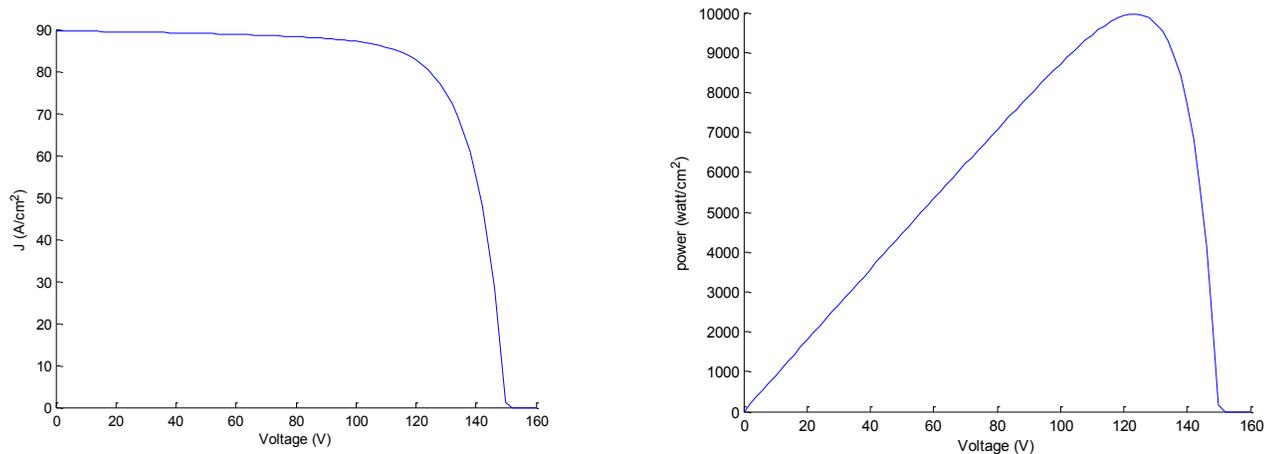

Figure 6.2: power vs voltage and current vs voltage curve

If we increase the number of parallel cell to 250 the series resistance will be = 4.8 ohm
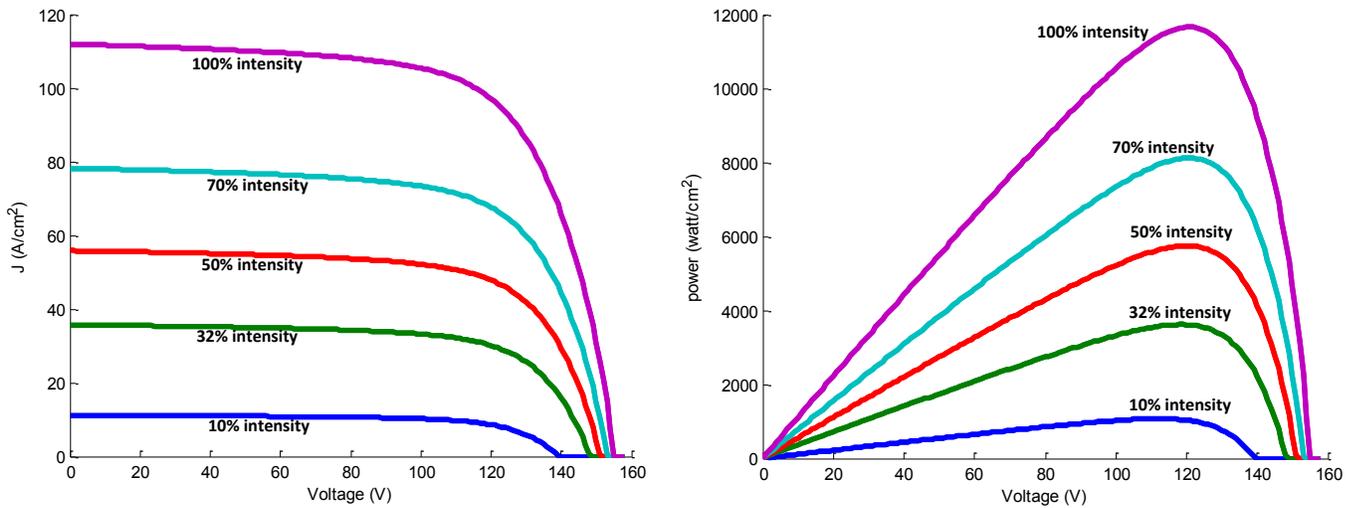
Figure 6.3: current vs voltage and power vs voltage and curve

The current and power-voltage characteristics of a CdTe solar cell by varying CdTe layer thickness is shown in Figure 6.4. All other parameters are kept same as the previous figures. However, the carrier lifetimes decreases with decreasing CdTe layer thickness. We can see the maximum power point shifts and are different in different CdTe layer thickness. If we compare the CdTe solar with a silicon solar cell as we did before in section 3.1 we can say that $J_L(V) \approx I_{pv,cell} \approx J_{sc}$. From equation (2.5), J_L increases with increasing W. And from the expression $V_{oc} \approx \frac{AkT}{e} ln \left[\frac{J_d}{J_0} \right]$ it is observable that V_{oc} also decreases with the increase of J_0 whereas J_0 is proportional to W. So, V_{oc} increases with decreasing W. However, the charge collection efficiency degrades with the CdTe layer thickness and hence, the *J-V* curves deviates from the rectangular shape and affects the solar cell efficiency.
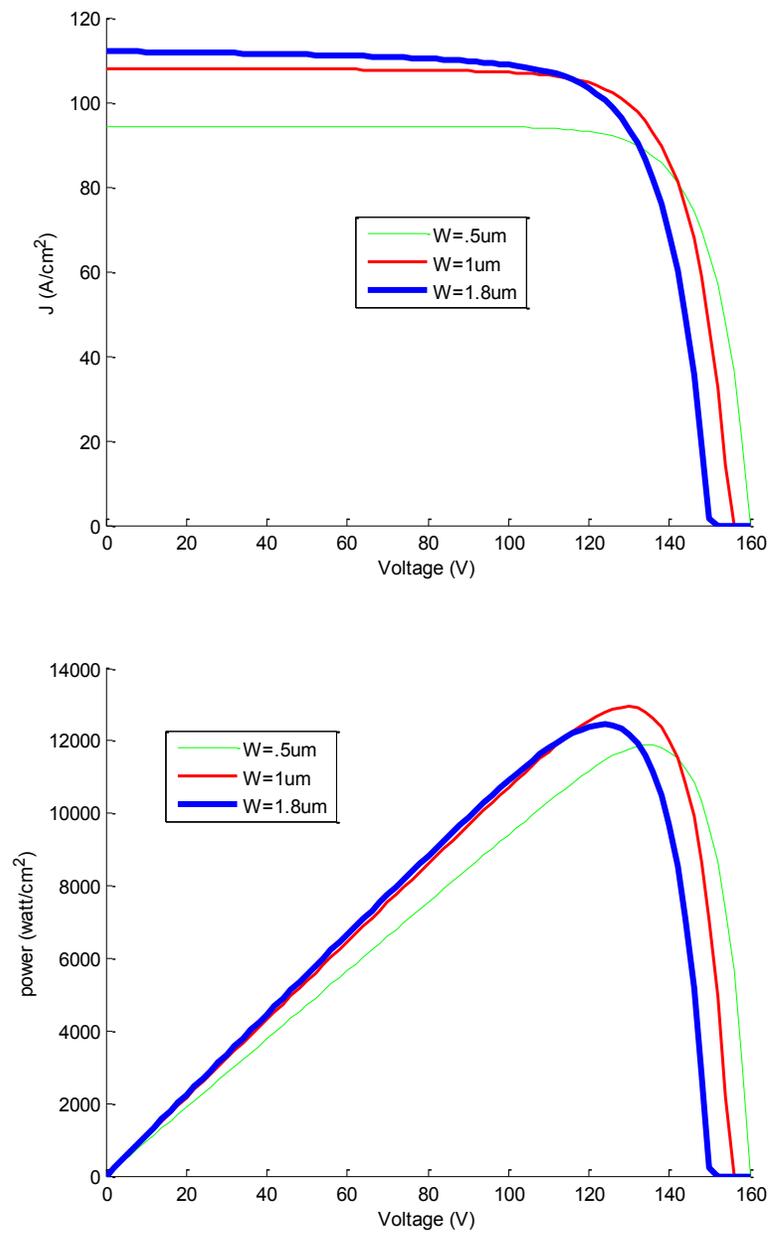
Figure 6.4: Current and Power - voltage characteristics of a CdTe solar cell varying CdTe layer thickness.

6.3 MPP effects for width change

We can see from the figure that the MPP changes responding to the change of CdTe width.

As the operating point should work always at MPP we can see width .5um gives us higher

voltage considering operating at the maximum power point. But if we increase the width, the operating current or the current delivered from the solar cell at MPP increases. So, there is a compromise whether manufacturing solar cell based on the purpose for which the solar would be used. If we need higher output voltage then definitely we should choose .5um. But if the system needs higher output current we choose 1.8um width solar cell.

## 6.4 Response to Maximum Power point tracking
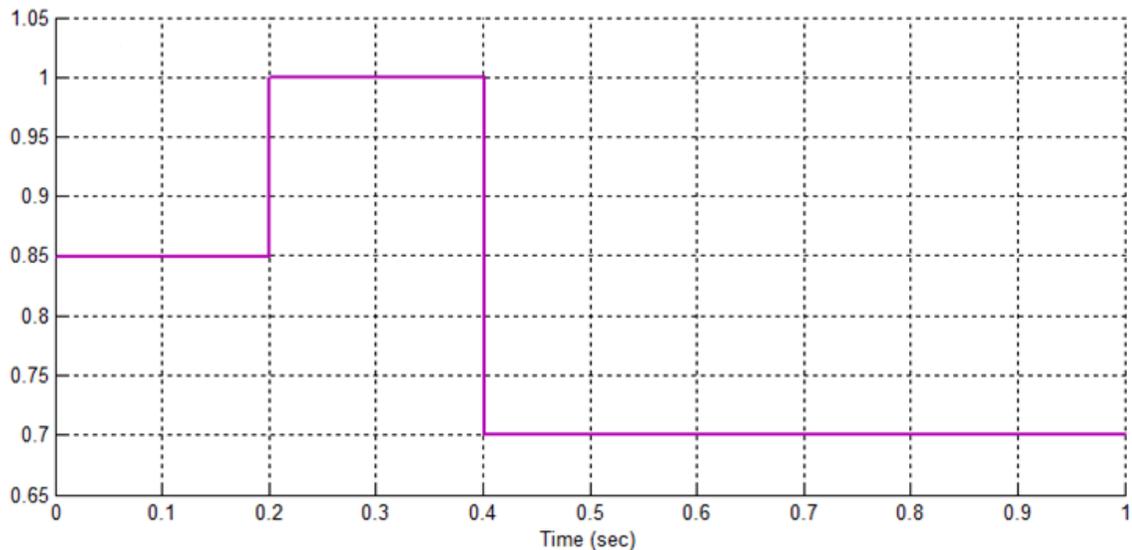
Figure 6.5: Change of intensity with time

Responding to the change in intensity, the power point shifts to the maximum point according to the algorithm presented in this paper, which is shown in Figure 6.6. The effects of temperature can also be included in the mathematical model described in section 6.5. When the temperature changes the maximum power point will shift and the circuit would operate at that point according to the Perturb and Observe algorithm applied.

68
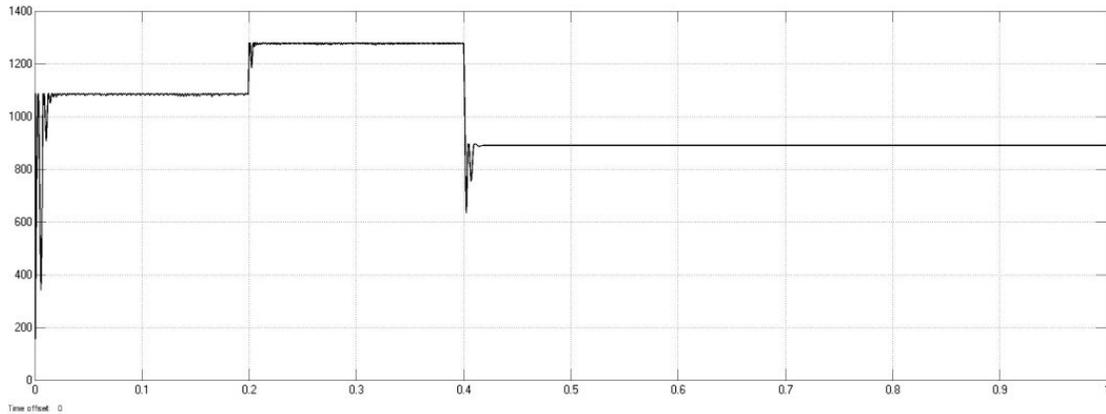
Figure 6.6: Circuits operate at MPP according to the algorithm as the intensity changes

For the charging a 24 kWh Li-ion battery with nominal voltage of 300V, 80Ah rated capacity is used to simulate the charging procedure. C/2 rate is used for constant charging. Figure 6.11 shows current profile during charging. Figure 6.12 shows battery voltage vs state of charge (SOC %).

6.5 Response to temperature change

The reverse saturation current J_0 given by Equation (2.11) is a function of n_i which is a strong function of temperature. With the increase in temperature the reverse saturation

current increases exponentially. Also from equation (2.10), the forward diode current J_d also related also increases exponentially with the temperature.
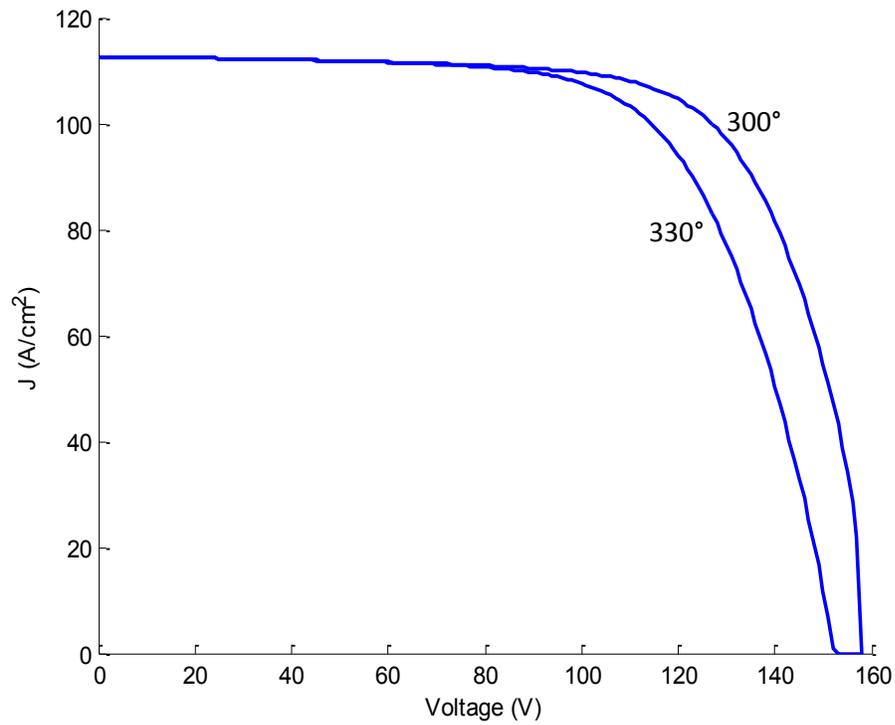

Figure 6.7: temperature effect on current voltage curve

As temperature increases less forward voltage is required to obtain the same diode current and the maximum power decreases as shown in Figure 6.7. If the voltage is held constant we can see that the diode current will increase with temperature. But the change in diode current is less sensitive than that in the reverse saturation current.
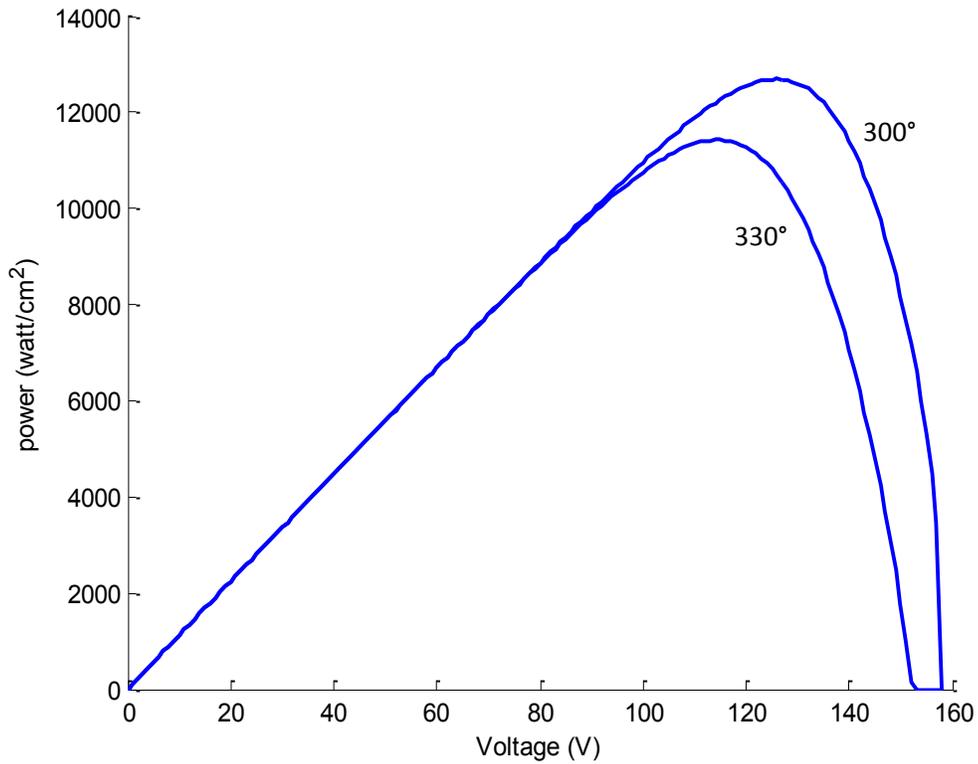
Figure 6.8: temperature effect on power curve

Also from the Figure 6.8 we can see that the maximum point change from one point to another. To introduce temperature effect we included n_i as function of temperature rather than using a constant value. For this we need to include the temperature dependent value of equilibrium concentration hence effective density state function N_C and N_V [42]. To do this we first derived the value of $N_C N_V$ from

$$N_c N_v =$$

$$n_i{}^2 exp\left[\frac{E_g}{kT}\right] \tag{6.2}$$

At T=300, $n_i = 2.23 \times 10^6 cm^{-3}$

Again N_C and N_V change with the temperature by

71

$$N_c = 2\left(\frac{2\pi m_n^* kT}{h^2}\right)^{3/2} \ and \ N_v = 2\left(\frac{2\pi m_p^* kT}{h^2}\right)^{3/2} \qquad (6.3)$$

So, $N_c \times N_v \propto T^3$

Therefore, finally n_i at T_1 temperature,

$$\frac{n_i^2 \times exp\left[\frac{E_g}{KT_1}\right]}{n_i^2{}_{T=300} \times exp\left[\frac{E_g}{KT_{T=300}}\right]} = \left(\frac{T_1}{300}\right)^3$$

$$=> n_i(T) = \left[(2.23 \times 10^6)^2 \times exp\left(\frac{E_g}{.0259}\right) \times \right.$$
$$\left.\left(\frac{T}{300}\right)^3 exp\left(\frac{-E_g}{KT}\right)\right]^{\frac{1}{2}} \qquad (6.4)$$

Here E_g is the direct band gap energy for CdTe material which is 1.5eV [43]. Figure 6.9 shows how the MPP changes with the temperature change. Figure 6.9 also contains the response of MPP change with the intensity.
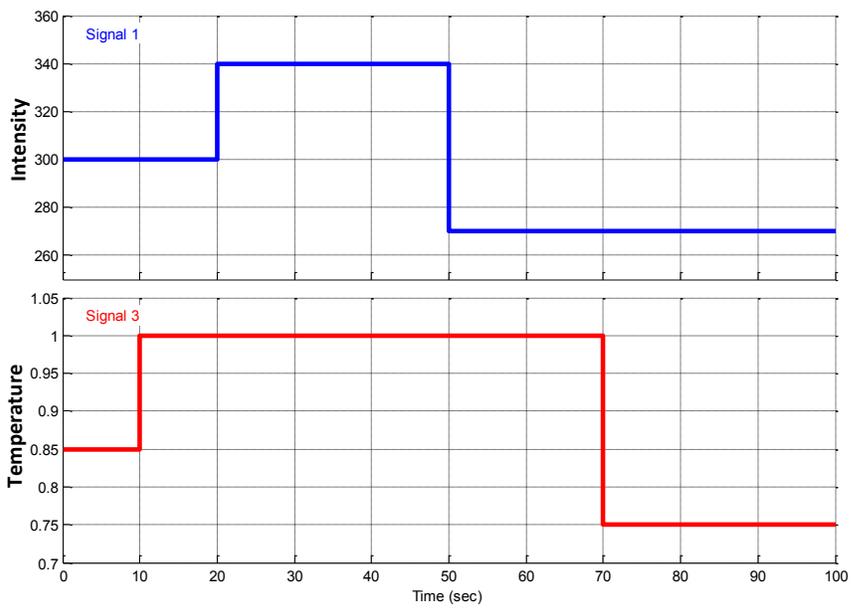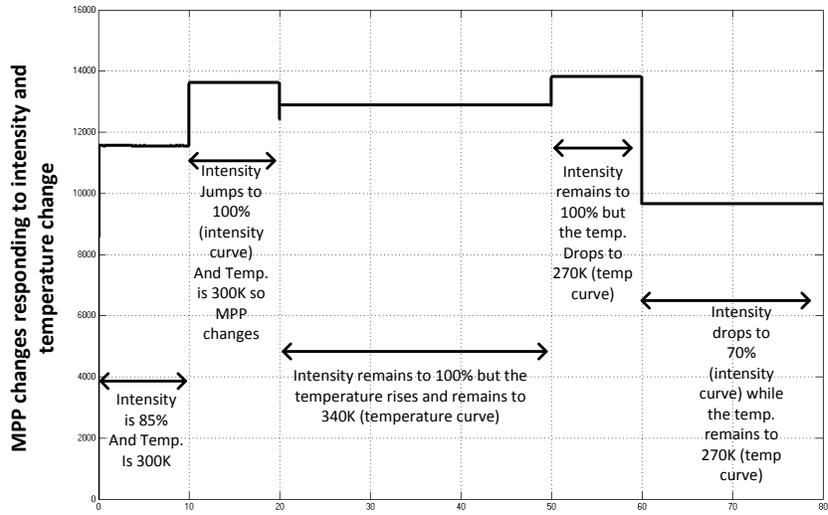
Figure 6.9: Maximum power point changes with the temperature and also with intensity change

6.6 Battery charging application simulation

A constant voltage (C-V) charger acts as a current source in an attempt to force the battery voltage up to a pre-set value usually referred to as the set-point voltage or set

voltage. Once this voltage is achieved, the charger would only provide enough current to hold the voltage of the battery at this constant voltage value. For this reason from this part it is called constant voltage charging.

The accuracy of the set point voltage is critical. Depending on taking the different preset value and by changing the battery parameter or changing capacitor or inductor value the charging profile may not show always the same as shown in Figure 6.11. But all the time, the charging always switches from CC to CV and the curve might be somewhat steep or wide. If the preset voltage is too high, the number of charging cycles the battery can complete, is reduced hence shortened the battery life. On the contrary if the preset voltage is too low, the cell will not be fully charged. In Figure 6.10 a typical charge profile for a Li-Ion cell using 1C constant current and constant voltage charging.
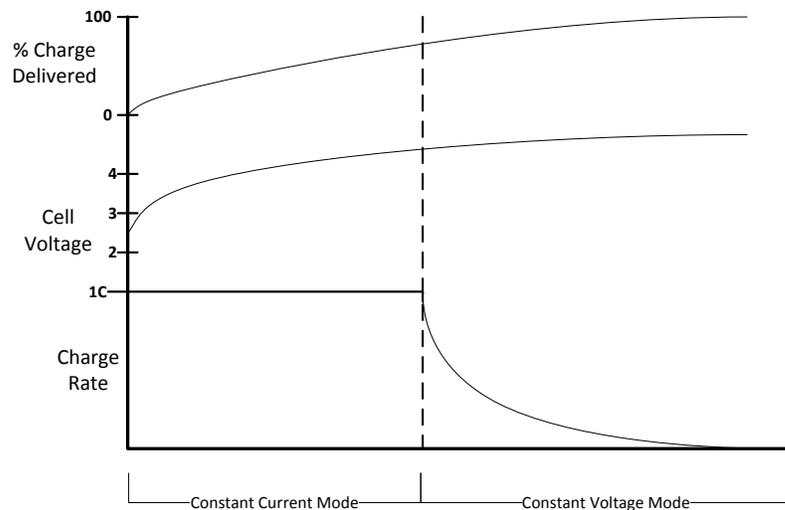

Figure 6.10: Typical C-V Charge Profile [32]

In our simulation for the charging a 24 kWh Li-ion battery with nominal voltage of 300V, 80Ah rated capacity is used to simulate the charging procedure. C/2 rate is used for constant charging. Figure 6.11 shows current profile during charging. Initial sate of charge

of the battery is taken as 89.8%. Figure 6.12 shows battery voltage vs state of charge

(SOC %). It resembles with a typical battery charging profile in Figure 6.10. The battery

voltage as a function of time is shown in Figure 6.13.
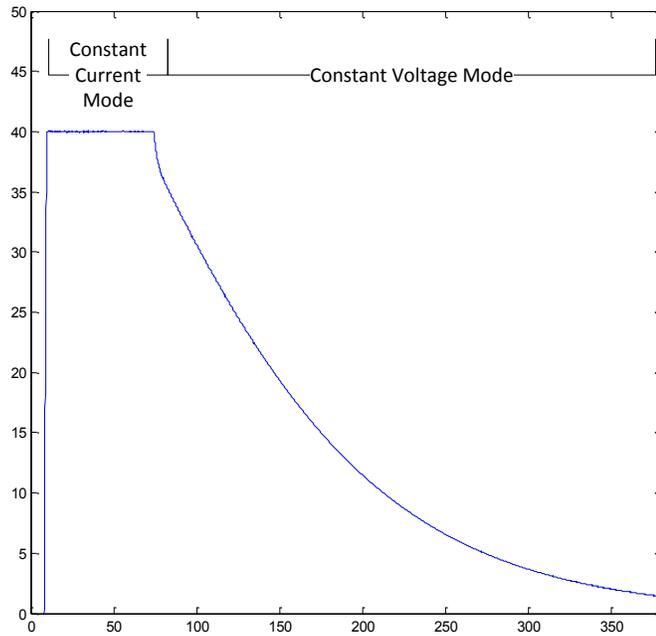
Figure 6.11: Current Vs time during battery charging
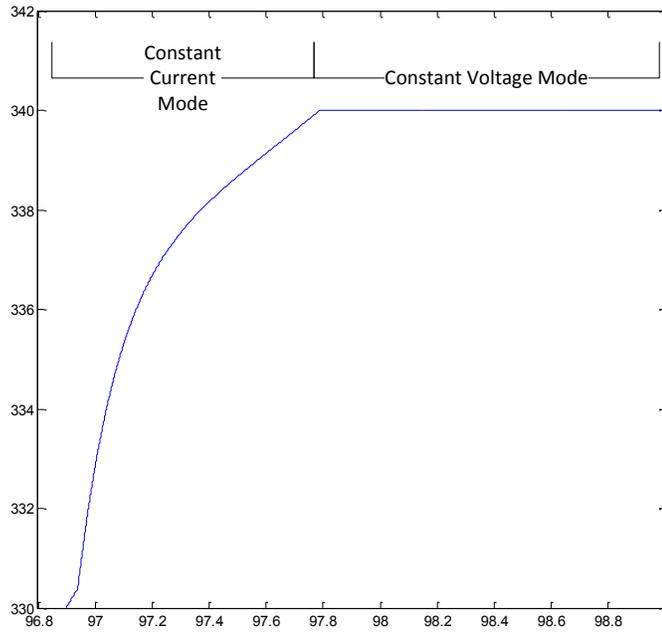
Figure 6.12: Voltage Vs SOC (%) profile
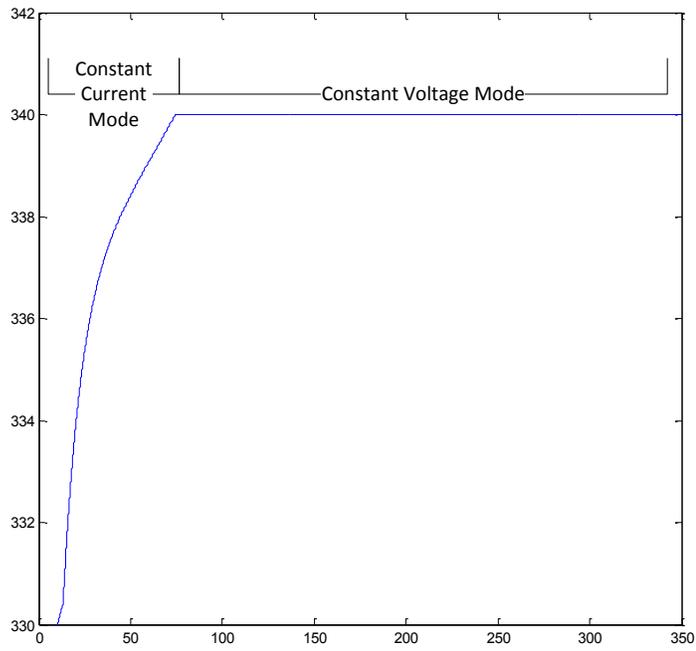
Figure 6.13: Voltage Vs time during battery charging

When there is unavailability of power during shading or other purpose the charging works in the constant current mode at different level or different low c-rate which is in acceptable range for charging. For example Figure 6.14 shows the intensity change and Figure 6.15 shows the different step charging current and voltage corresponding to different intensity.
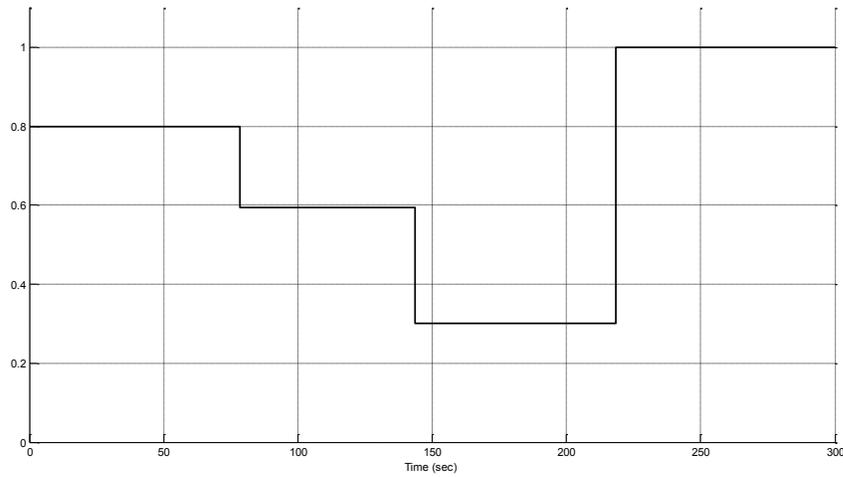
Figure 6.14: Intensity change to see the behavior of charging current at low intensity
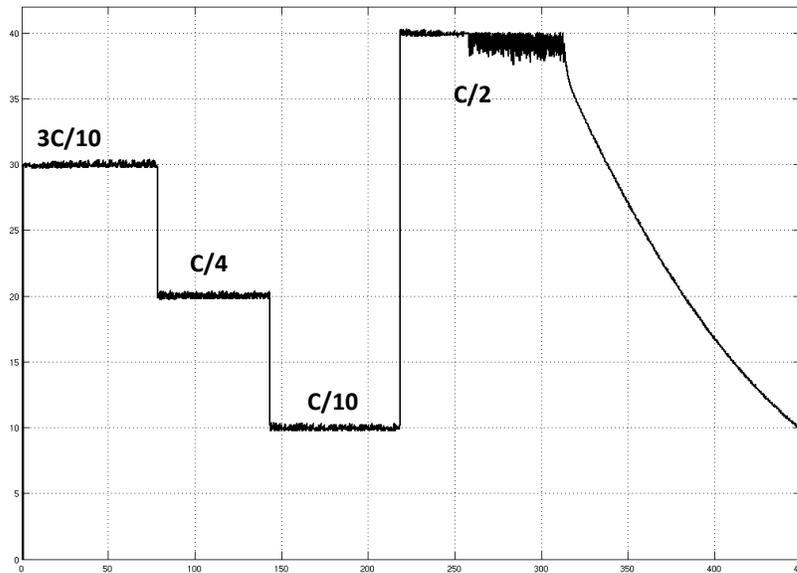
Figure 6.15: Charging current in different intensity; C/10 constant current in intensity as low as 30%

We can see from the figure that during intensity as low as 30% the charging system switch to C/10 constant charging rate where the operating point of the solar cell also shifts to maximum power point corresponding to different intensity. The simple switch mode converter, i.e., the same two quadrant dc-dc buck converter is used for working all the modes whether it is CC or CV. Battery would be disconnected if there is over charge or over discharge. Both the converters (used for MPP tracking) and battery charging use algorithm driven adjustable duty cycle switching that is capable of switching between CC and CV when needed.

A 3-stage constant current and constant voltage (CC-CV) process can also be applied for Lithium-ion chargers to charge a rechargeable battery, [44] as shown in
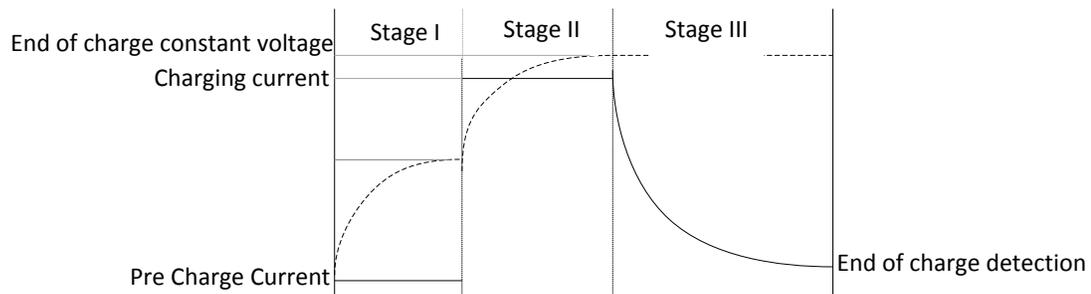
Figure 6.16: Power curves for different types of thin film solar cells

A pre-charged stage known as trickle charge is applied to take the battery to a preset value which is heavily discharged before applying that charge. In phase I, the battery is charged with a low current rate until the battery voltage reaches a threshold value to switching mode. It minimizes heat dissipation by avoiding the battery to charge with a high current rate when the internal resistance of the battery is low at the initial stage. In phase

II, a higher constant current rate is used to charge the battery till a pre-defined voltage level is reached, then a constant voltage mode is applied until the end of charge trigger condition is matched. The termination condition is set either when the charge current rate is below a pre-defined small value or the measured temperature is over a preset temperature which is described in battery charging basic sections. The CV mode is to avoid over potential charging which can damage the battery cycle life [31]. In phase III we can see the exponential decreasing of the charge current. Constant current portion can be modeled with multistep constant current charging as it has been shown and proposed in [45] [46] for lead-acid and nickel/metal hybrid batteries.

**6.6 Comparing CdTe solar cell with other thin film solar cells**
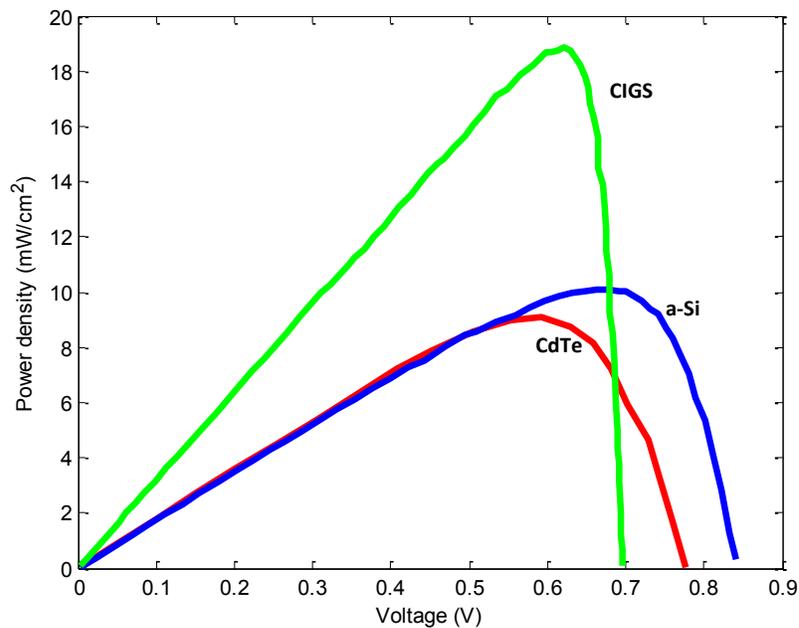
Figure 6.17: Power curves for different types of thin film solar cells
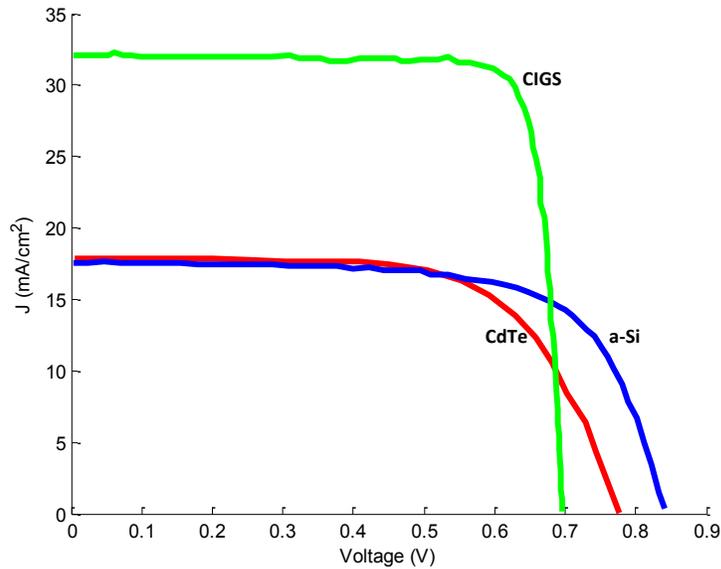
Figure 6.18: current voltage characteristics for different types of thin film solar cells

Figures 6.17 and 6.18 are showing the power and J-V characteristics of different thin film solar cells. The data are extracted from Ref [3] and Ref [47]. For CdTe and a-Si we can see the MPP occurs in the range of 8mW to 10mW. And for CIGS it occurs at 19mW. Though the current for the CIGS cells is very high the voltage for MPP are almost the same. So, the effect of series resistance when increasing the voltage by adding series cells is almost the same for all three thin films. However the number of parallel cells would be significantly reduced for CIGS solar cell when forming solar network to deliver a specific charging current to charge a battery. However, if we think of production cost, we can see for CdTe solar cell, it is now .8/Watt and it will be reduced in near future, for a-Si the cost is \$1.06/Watt and for CIGS it is around \$1.12/Watt. Therefore, for EV opportunity charging where thousands of charging stations on the driveway could be a way to attract the EV customers, definitely CdTe solar network would be a good option instead of using the costly solutions.

80

Chapter 7: Conclusion, Contributions, Publications and Futures Works

7.1 Conclusion

Recent days the efficiency of the CdTe solar cell has reached to 17.3 % where it's the lowest quoted thin-film module price stands at US$0.84 per watt-peak, comparing to the lowest quoted crystalline silicon (c-Si) module at $1.06 per watt-peak [48]. Though the production of solar cells is still based mainly on crystalline silicon (Si), we can see the market share of thin film solar increases over the last few years. Among the thin film solar cells the most common materials used are amorphous silicon (a-Si) and the polycrystalline materials that includes cadmium telluride (CdTe), copper indium (gallium), and di-selenide (CIS or CIGS) [48]. Each of these materials can be deposited over a large area, and hence can be used for high volume manufacturing. In this paper this promising CdTe solar cell has been analyzed and simulated with one of its very important application. Perturb and Observed algorithm maximum power point technique is developed and used with the dc-dc boost converter to extract maximum power. Then a bi-direction two quadrant dc-dc buck converter is followed to charge a 24 kWh Li-ion battery. Charging algorithm drives the dc-dc converter in constant current and constant voltage mode as needed. Maximum power point tracking as well as constant current charging behavior are observed and analyzed in different intensity and temperature. Methods for designing the converters for MPPT and specific charging characteristics are also disclosed and discussed. Both the MPP and charging algorithms work consistently without showing any mismatch regardless of changing from one MPP to another or one mode to another or even disconnecting the battery.

7.2 Contributions

- First of all, in this thesis, a multidisciplinary interface approach is integrated to analyze for CdTe solar cell application for battery charging.

- Both the MPPT and charging algorithms work consistently without showing any mismatch. The linking between MPPT and the charging system has been done by allowing the range of operation of the converters in such a way that the boost converter can work in the MPP while the buck converter can charge the battery in wide ranges. If completely two separately designed systems, i.e., charging and MPPT are combined together they might show mismatch for several reasons. There are not many descriptions to describe the reason behind this in the literature. But one of the reasons might be when they were designed separately; the duty cycle of the converter of one system is allowed to work only in a small window not considering the other system. But when they were designed in combined, the DC link voltage is also important because there is no usual load but the battery. Also one important point needs to mention that, the battery that has been used in this simulation is not a stationary battery but an EV standard Li-ion battery. For stationary battery, like Lead acid that can provide as much power as an EV needs can be charged with a simple constant voltage charging. But that battery would never be mobile but a stationary one. So, for stationary battery constant voltage part of the algorithm can be easily utilized and in that way the use of the algorithm can be extended to charge stationary batteries which are being used powering the house or buildings. Also the charging system can be used to charge battery in the parking lot or garage from the PV panels that are already being attached with the buildings to supply power for housings and others.

7.3 Publications

1. **K. N. Sakib**, M. Z. Kabir, and S. S. Williamson, "Simulation of Battery Charging Application from Cadmium Telluride Solar Cell Modeling," in Proc. *Annual Conf. of the IEEE Industrial Electronics Society*, Vienna, Austria, Nov. 2013.

2. **K. N. Sakib**, M. Z. Kabir, and S. S. Williamson, "Cadmium Telluride Solar Cell: From Device Modeling to Electric Vehicle Battery Management," in Proc. *IEEE Transportation Electrification Conf. & Expo.*, Detroit, MI, June 2013.

3. **K. N. Sakib**, M. Z. Kabir, and S. S. Williamson, "Cadmium Telluride Solar Cell: From Device Modeling to System Implementation," in Proc. *IEEE International Conf. on Industrial Technology*, Cape Town, South Africa, Feb. 2013.

7.4 Future Works

- The single cell is verified with the experimental data. The array model can be verified with experimental data. In that case a module or a network of modules needs to buy. Then it can be verified by varying the load to extract the different experimental data points.

- The algorithm can be upgraded to multi stage constant current mode and also with also several charging stages as shown in **Error! Reference source not found.**Figure 6.16. The algorithm is made simple to include this several stage by introducing similar numbers of decision making step after determining the V_{ref} step as shown in
- Figure 5.1.

- The temperature effect can be made more sensitive to temperature response by introducing a band gap energy modeling for CdTe solar cell as the band gap is not completely constant with the temperature as we took in our model.

References

[1] A. Wolden, J. Kurtin, J.B. Baxter,I. Repins, S. E. Shaheen, J.T. Torvik, A.A. Rockett, V. M. Fthenakis,E. S. Aydil, "Photovoltaic manufacturing: Present status, future prospects, and research needs" J. Vac. Sci. Technol. A 29(3), pp.1-16, 2011

[2] J. Nelson, "The physics of solar cells" (Imperial College Press, London, 2003), chapter 8.

[3] S. S. Hegedus and W. N. Shafarman, Thin-film solar cells: device measurements and analysis, Prog. Photovolt: Res. Appl., 12, pp. 155, 2004.

[4] S. S. Hegedus, Current-Voltage Analysis of a-Si and a-SiGe Solar Cells Including Voltage-dependent Photocurrent Collection Prog. Photovolt: Res. Appl., **5**, pp. 151, 1997.

[5] Martin A. Green, ARC Photovoltaic Centre of Excellence, University of New South Wales, Thin-film solar cells: review of materials, technologies and commercial status, Springer Science & Business Media, LLC 2007. , Published online: 3 April 2007

[6] P. Mints, Analysis of Worldwide PV Markets and Five-Year Application Forecast 2009/2010 Navigant Consulting, San Francisco, CA, 2010

[7] Concentrator Photovoltaic (CPV) Workshop, October 17, 2011, Dallas, Texas

[8] J. Poortmans and V. Arkhipov (eds.), Thin Film Solar Cells: Fabrication, Characterization and Applications (Wiley & Sons, Chichester, 2006)

[9] X. Wu, R.G. Dhere, D.S. Albin, T.A. Gessert,C. DeHart, J.C. Keane, A. Duda, T.J. Coutts, S. Asher, D.H. Levi, H.R. Moutinho, Y. Yan, T. Moriarty, S. Johnston, K. Emery and P. Sheldon, "High-Efficiency CTO/ZTO/CdS/CdTe Polycrystalline Thin-Film Solar Cells" 14-17 October 2001

[10] Enoki Chen, Digitimes Research: GE, First Solar improving CdTe thin-film solar cell efficiency, Taipei, April 11 2013

[11] Richard Stevenson, First Solar: Quest for the $1 Watt, "First Solar: Quest for the $1 Watt", IEEE Spectrum, August 01, 2008

[12] C. C. Chan, "The State of the Art of Electric, Hybrid, and Fuel Cell Vehicles range requirement in real-world driving", Proceedings of the IEEE, Volume: 95, pp: 704-718, April 2007

[13] Andrew F. Burke, "Batteries and Ultracapacitors for Electric, Hybrid, and Fuel Cell Vehicles", Proceedings of the IEEE", Volume: 95 pp: 806-820, April 2007

[14] Ali Emadi, Kaushik Rajashekara, Sheldon S. Williamson and Srdjan M. Lukic, "Topological Overview of Hybrid Electric and Fuel Cell Vehicular Power System Architectures and Configurations", IEEE Transactions on vehicular technology, vol. 54, no. 3, pp: 763-769, May 2005

[15] I.J.M. Besselink, P.F. van Oorschot, E. Meinders, H. Nijmeijer, "Design of an efficient, low weight battery electric vehicle based on a VW Lupo 3L", The 25th World Battery, Hybrid and Fuel Cell Electric Vehicle Symposium & Exhibition, EVS-25 Shenzhen, China, Nov. 5-9, 2010

[16]   Mishra, P., Pandey, A., and Joshi, J.: 'Design of a battery voltage regulator based on maximum power point tracking and charge equalisation concepts', Sol. Energy Mater. Sol. Cells, 44 ,(1), pp. 11–24, 1996

[17]   T. Esram, and P. L. Chapman, "Comparison of Photovoltaic Array Maximum Power Point Tracking Techniques," IEEE Trans Energy Conversion, vol. 22, pp. 439-449, 2007.

[18]   S. S. Kondawar and U. B. Vaidya, "A Comparison of Two MPPT Techniques for PV System in Matlab Simulink", International Journal of Engineering Research and Development, vol. 2, pp. 73-79, 2012.

[19]   M. S. Anjan and M. Z. Kabir, "Modeling of the current-voltage characteristics of CdS/CdTe solar cells", Physica Status Solidi A, 208, pp. 1813-1816, 2011.

[20]   C. T. Sah, R. N. Noyce, and W. Shockley, "Carrier generation and recombination in p-n junctions and p-n junction characteristics," Proc. IRE 45, pp. 1228, 1957.

[21]   Steven Hegedus, Darshini Desai and Chris Thompson, "Voltage dependent photocurrent collection in CdTe/CdS solar cells", Prog. Photovolt: Res. Appl., 15, pp. 587-602, 2007 and references therein.

[22]   D A Wood, K D Rogers, D W Lane† and J A Coath, Optical and structural characterization of CdS_xTe_{1-x} thin films for solar cell applications

[23]   American Society for Testing and Materials (ASTM) Terrestrial Reference Spectra for Photovoltaic Performance Evaluation , April, 2013

[24] Marcelo Gradella Villalva, Jonas Rafael Gazoli, and Ernesto Ruppert Filho, "Comprehensive Approach to Modeling and Simulation of Photovoltaic Arrays", IEEE Transactions on power electronics, vol. 24, no. 5, pp. 1198-1206, may 2009

[25] A. N. Tiwari, G. Khrypunov, F. Kurdzesau, D. L. Ba¨tzner, A. Romeo and H. Zogg, "CdTe Solar Cell in a Novel Configuration", Progress in Photovoltaics: Research and Applications, Vol. 12, pp. 33–38, January 2004.

[26] Antonio Luque Instituto de Energ´ıa Solar, Steven Hegedus, "Handbook of Photovoltaic Science and Engineering, Second Edition", A John Wiley and Sons, Ltd., Publication, 2011

[27] T.Chaitanya, Ch.Saibabu, J.Surya Kumari, "Modeling and Simulation of PV Array and its Performance Enhancement Using MPPT (P&O) Technique", International Journal of Computer Science & Communication Networks,Vol 1(1) pp. 9-15, September-October 2011

[28] Isidor Buchmann, Batteries in a Portable World, Cadex Electronics Inc.; 3rd edition (April 11, 2011)

[29] Rechargeable Batteries Applications Handbook – pp. 186

[30] Johann Dussarrat, Gael Balondrade, Design of a Test Bench for Battery Management Report Performed at Electronic Devices at Linköping Institute of Technology

[31] D. Linden, Handbook of Batteries, 3rd ed. McGraw-Hill, 2002.

[32]   Chester Simpson, Battery Charging, National Semiconductor, Texus Instrument, Literature Number: SNVA557

[33]   L. J. Curran, "Charger ics reflect shift to smart batteries," EDN (Electronics Design Network), pp.10–11, 1997.

[34]   R. Schweber, "Supervisory ics empower batteries to take charge," EDN, pp. 61–72, September 1997.

[35]   Harrington, S., and Dunlop, J.: 'Battery Charge Controller Characteristics in Photovoltaic Systems', IEEE Aerosp. Electron Syst. Mag., Vol. 7, pp. 15–21, August 1992,

[36]   James P. Dunlop, "Batteries and charge control in stand-alone PV fundamentals and applications", publication number FSEC-CR-1292-01, Florida Solar Energy Center, pp. 41-43, January 15, 1997

[37]   Duryea, S., Islam, S., and Lawrance, W.: 'A battery management system for standalone photovoltaic energy systems'. Proc. 34th Annual Meeting of the IEEE Industry Applications Conf., Phoenix, USA, Vol. 4, pp. 2649–2654, 1999.

[38]   Hruska, Louis W. , Smart batteries and lithium ion voltage profiles, Battery Conference on Applications and Advances, Twelfth Annual conference, pp. 205-210, 14-17 Jan, 1997

[39]   Erickson, R. W., "DC–DC Power Converters", article in Wiley Encyclopedia of Electrical and Electronics Engineering, Vol. 5, pp. 53-63, 1999

[40]   M. Miyake, K. Murase, T. Hirato, Y. Awakura, "Hall effect measurements on CdTe layers electrodeposited from acidic aqueous electrolyte" J. Electroanal. Chem. vol. 562, pp. 247-253, 2004.

[41]   W.K. Metzger, D. Albin, D. Levi, P. Sheldon, X. Li, B. M. Keyes, and R. K. Ahrenkiel, "Time-resolved photoluminescence studies of CdTe solar cells" J.Appl. Phys., 94, 3549, 2003.

[42]   Donald A. Neaman, Semiconductor physics and basic principal 3rd Edition, University of New Maxico, pp. 102-115, 2003

[43]   K. L. Chopra, P. D. Paulson, y and V. Dutta, Photovoltaic Laboratory, Centre for Energy Studies, Indian Institute of Technology Delhi, Thin-Film Solar Cells: An Overview, Prog. Photovolt: Res. Appl. vol. 12, pp. 69–92, May, 2004

[44]   Lan-Ron Dung and Jieh-Hwang Yen Dept. of Electr. & Control Eng., Nat. Chiao-Tung Univ., Hsinchu, Taiwan, ILP-Based Algorithm for Lithium-Ion Battery Charging Profile, Industrial Electronics (ISIE), 2010 IEEE International Symposium, pp. 2286 - 2291, 4-7 July 2010

[45]   T. Ikeya, N. Sawada, S. Takagi, J. Murakami, K. Kobayashi, T. Sakabe, E. Kousaka, H. Yoshioka, S. Kato, M. Yamashita, H. Narisoko, Y. Mita, K. Nishiyama, K. Adachi, and K. Ishihara, "Multi-step constant-current charging method for an electric vehicle, valve-regulated, lead-acid batteries during night time for load-leveling," Journal of Power Sources, vol. 75, no. 1, pp. 101–107, September 1998.

[46]   T. Ikeya, N. Sawada, J. Murakami, K. Kobayashi, M. Hattori, N. Murotani, S. Ujiie, K. Kajiyama, H. Nasu, H. Narisoko, Y. Tomaki, K. Adachi, Y. Mita, and K. Ishihara, "Multi-step constant-current charging method for an electric vehicle nickel/metal hybrid battery with high-energy efficiency and long cycle time," Journal of Power Sources, vol. 105, no. 1, pp. 6–12, March 2002.

[47]   E. Klimovsky, J.K. Rath, R.E.I. Schropp, F.A. Rubinelli, "Modeling a-Si:H p–i–n solar cells with the defect pool model", J. non-crystalline Solids, 338–340, 686–689, 2004.

[48]   Solar market research and analysis report by "NPD Solarbuzz", April, 2013.